Targeting Neuropilin-1 to Enhance Immunotherapy in Melanoma: Reducing Tumour Progression and Peripheral Treg-Mediated Immunosuppression.

Somlata Khamaru[a,b#], Kshyama Subhadarsini Tung[a,b], Subhasis Chattopadhyay[a,b*]

[a]National Institute of Science Education and Research, School of Biological Sciences, Bhubaneswar, Odisha 752050, Odisha, India.

[b]Homi Bhabha National Institute, Training School Complex, Anushaktinagar, Mumbai, 400094, India.

***Correspondence:**

Subhasis Chattopadhyay, School of Biological Sciences, National Institute of Science Education and Research, PO- Bhimpur-Padampur, Via- Jatani, Khurda-752050, Odisha, India. Tel- 0674-2494201. E-mail address: subho@niser.ac.in

Abstract

Melanoma, the most aggressive form of skin cancer with a high mutation rate, is the fifth most common cancer among Caucasians. Despite advancements in treatments like immune checkpoint inhibitors and targeted therapies, over 40% of patients experience immune-related adverse events, posing significant challenges. Neuropilin-1 (NRP1) has emerged as a critical immune-oncology target due to its overexpression in multiple cancers, where it enhances regulatory T cell (Treg) function and promotes tumour progression, often leading to a poor prognosis.

This study explored the effects of NRP1 inhibition in B16-F10 melanoma and its impact on peripheral Treg-mediated immune responses. NRP1 was overexpressed in several cancers, including B16-F10 cells, compared to non-tumorigenic NIH-3T3 cells. It inhibited NRP1 selectively induced apoptosis in B16-F10 cells without affecting NIH-3T3 cells. It also reversed the immunosuppression of splenic T cells induced by B16-F10-conditioned supernatants *in vitro* by reducing suppressor T cell markers (NRP1, NKG2A, FOXP3), Treg activity, and secretion of immunomodulatory cytokines (IL-10, IL-17A). Additionally, NRP1 inhibition increased T cell proliferation and enhanced effector cytokine responses (TNF, IFN-γ, IL-6, IL-2). NRP1 inhibition also downregulated the STAT, ERK MAPK, and Smad2/3 pathways while upregulating the PI3K/AKT pathway. In splenic T cells isolated from B16-F10 tumour-bearing mice treated with an NRP1 inhibitor, there was a reduction in immunosuppressive T cell marker expression and Treg suppressive activity, alongside an increase in T cell proliferation. NRP1 inhibitor treatment also significantly reduced lung metastasis, decreased tumour volume, and improved survival rates in these mice.

This study demonstrates that NRP1 inhibition may help reduce B16-F10 melanoma progression and associated peripheral Treg-mediated immunosuppression, highlighting its potential in developing future anti-cancer immunotherapy strategies, particularly in combination therapies.

Introduction

Melanoma, a perilous skin cancer arising from uncontrolled melanocyte growth, has been the most lethal form of skin cancer. Its incidence has surged dramatically over the past 50 years, particularly among Caucasians, causing substantial health and economic impacts due to the high average years of life lost per death (1).

Melanoma, an immunogenic tumour, has a worse prognosis under immunosuppressive conditions. Several studies identified various mechanisms of melanoma-induced immunosuppression: down-

regulation of surface antigens, mutations, lack of costimulatory function, recruitment of immunosuppressive cells, secretion of immunosuppressive cytokines, and induction of tolerance. According to earlier studies, regulatory T cells (Tregs) ($CD4^+CD25^+$ $FOXP3^+$) were linked to poor immunotherapy responses and were more prevalent in advanced melanoma (2–4). Increased expression of programmed cell death 1 protein (PD-1) in melanoma-specific $CD8^+$ T cells has been reported to lead to higher apoptosis rates of these cells, impairing their antitumour response (5). In melanoma, PD-1 on cytotoxic T-lymphocytes was reported to interact with programmed death ligand 1 (PD-L1) on tumour and immune cells (dendritic cells (DCs) and other antigen-presenting cells (APCs)), leading to T-cell exhaustion (6). Earlier reports also suggested that other checkpoints such as Neuropilin-1 (NRP1), cytotoxic T-lymphocyte associated protein 4 (CTLA-4), T-cell immunoglobulin and mucin-domain containing-3 (TIM-3), lymphocyte-activation gene 3 (LAG-3) and V-domain immunoglobulin suppressor of T cell activation (VISTA), suppressed T-cell activity and facilitated tumour proliferation and metastasis (7–18). Previous reports also suggested that Tregs recruited in the melanoma microenvironment modulate immunity through cytokine release (interleukin-10 (IL-10), interleukin-35 (IL-35), transforming growth factor beta (TGF-β)), cytotoxicity against T cells, inhibition of DC maturation, and metabolic disruption (16,19). Melanoma was also reported to block natural killer (NK) cell responses through ligands like Fas, apoptosis antigen 1 (APO1), and Natural Killer Cell Receptor (NKG2A) ligands that induced apoptosis of immune effector cells (2). Additionally, melanoma cells were reported to secrete factors like vascular endothelial growth factor (VEGF), TGF-β, essential fibroblast growth factor (bFGF), galectins, Th_2 cytokines, chemokines, indoleamine 2,3-dioxygenase (IDO), exosomes that facilitate in inducing peripheral tolerance and immunosuppression (20).

Immune checkpoint inhibitors (ICIs), such as anti-CTLA-4 and anti-PD-1 antibodies, were reported to target the dysfunctional immune system to induce the killing of cancer cells by $CD8^+$ T cells, achieving significant tumour regression and long-term control in nearly 50% of advanced melanoma patients, compared to less than 10% historically (12). However, studies depicted that approximately half of the patients did not experience lasting benefits, even with combination immune-checkpoint inhibitors (ICIs) (21). Earlier studies suggested immunoresistance to ICI-based therapy involves genomic and immune system cell-related factors, the cancer microenvironment, host factors, age, sex, diet, hormones, comorbidities, and the gut microbiome (22). ICIs were reported to cause immune-related adverse events (irAEs) and are costly, necessitating targeted use to maximise benefits and minimise costs. Identifying biomarkers that predict response and severe side effects is crucial for optimising cancer therapy (11,23). Interestingly, checkpoint blockade therapy reversed T cell inhibition through inhibitory receptors (IRs) such as LAG-3 and TIM-3, highlighting the

importance of balance between effector T cell activation and suppressor Treg cells post-administration. Tailoring therapies based on this balance could optimise clinical outcomes for specific malignancies and individual patients (23).

Neuropilin, a type I transmembrane protein with two homologues, Neuropilin-1 (NRP1) and Neuropilin-2 (NRP2), acts as a receptor for class 3 semaphorins (Sema3A) and specific VEGF isoforms (24). Recently, NRP1 has gained attention in immune-oncology to enhance Treg cell suppression and limit durable effector T cell responses. Initially identified as a Treg cell marker, NRP1 stabilised Tregs in the tumour microenvironment (TME), inhibiting CD8+ T cell anti-tumour activity. In cancer, NRP1 on Tregs promoted immune suppression by facilitating Treg recruitment via VEGF co-receptor activity and maintaining tumour-specific Treg stability through Sema4a binding, which also facilitated survival and function of these Tregs through modulation of the Akt-mTOR signalling and PTEN-Akt-FoxO axis (25,26). Elevated $NRP1^{+}$ Tregs underscored its critical role in immune regulation within tumours (23). Additionally, reports suggested NRP1 as an emerging therapeutic target in malignant melanoma, aiming to reduce invasiveness, counteract serine/threonine-protein kinase B-Raf (BRAF) inhibitor resistance, inhibit Treg recruitment, and synergise with immunotherapies to delay tumour progression and resistance development (27). Furthermore, earlier reports showed that when anti-NRP1 was combined with anti-PD-1 immunotherapy, it enhanced CD8+ T cell proliferation, cytotoxicity, and tumour control. Hence, targeting NRP1 in combination with immunotherapy may be a promising approach (28).

Overall, leveraging NRP1 biology for cancer therapeutics showed promise, especially in combination with immunotherapies and not directly targeting Treg cell function. Understanding NRP1's role across the TME is crucial for designing optimal clinical strategies with this immune modulator. Inhibition of NRP1 by depletion, knockout, inhibitors, monoclonal antibodies, and nanobodies has significantly reduced angiogenesis, tumorigenesis, tumour growth, and metastasis and improved survival (7,23,28–37). Although inhibitors and microRNAs have been reported to exhibit anti-cancer activity by inhibiting NRP1, EG00229 is identified as the most specific NRP1 inhibitor to date (28). It has been reported to inhibit NRP1's interaction with VEGFA, showing significant tumour-suppressive effects in cholangiocarcinoma, lung adenocarcinoma, gliomas, and squamous cell carcinomas (38–42). While NRP1 is a potential target for melanoma and repurposed drugs against melanoma have been studied (43,44), EG00229's anti-tumour activity on melanoma remains unstudied. Furthermore, although NRP1 depletion and inhibition in cancer cells and intra-tumoral Tregs have shown favourable anti-tumour immune responses (36,37,45), the study of NRP1 depletion/inhibition in peripheral Tregs and its subsequent anti-tumour activity is albeit scanty (35),

yet promising. Also, the potential anti-tumour role of EG00229 has been studied in different cancers (41,46,47), but its effect on Tregs (intratumoral or peripheral) remains unexplored.

Accordingly, in the current study, Treg-mediated regulation of B16-F10 melanoma-driven immunosuppression of peripheral splenic T cells, underlying cellular pathways, impact on IRs and the subsequent anti-tumour response upon inhibition of NRP1 with EG00229 trifluoroacetate (EG), has been delineated. This translational mechanistic insight might aid in the implications of NRP1 as a pivotal checkpoint in the peripheral Tregs and a promising anti-cancerous immunotherapeutic target, either alone or in combination with current standard therapeutic regimens.

Materials and Method

Cell lines:

The murine melanoma cell line B16-F10 (ATCC™ CRL-6475™) and the murine fibroblast cell line NIH-3T3 (ATCC™ CRL-1658™) were cultured in Dulbecco's Modified Eagle's Medium (DMEM; Gibco, Grand Island, New York) supplemented with 10% fetal bovine serum (FBS; Gibco), 1X antibiotic solution (100X Liquid, HiMedia Laboratories Pvt. Ltd., Mumbai, India), and 1X L-glutamine (HiMedia). The cells were incubated at 37°C in a humidified CO_2 incubator. For passaging, 1X trypsin solution (HiMedia) was used for both B16-F10 and NIH-3T3 cells.

Antibodies and Reagents:

PE Annexin V Apoptosis Detection Kit I, purified NA/LE Hamster Anti-mouse CD3e (cat no.-567114) and CD28 (cat no.-553294) antibodies, fluorophore-conjugated anti-mouse CD3 (cat no.-553062), CD279 (PD-1, cat no.-J43), CD274 (PD-L1, cat no.-M1H5), NKG2AB6 (cat no.-16a11), CD152 (CTLA-4, cat no.-UC10-4F10-11), CD4 (cat no.-GK1.5) antibodies were from BD Biosciences (SJ, USA). Fluorophore-conjugated anti-mouse CD304 (NRP1, cat no.- 25-3041-82), FOXP3 (cat no.-FJK-16s), GATA-3 (cat no.-TWAJ) and T-bet (4B10) antibodies, Dynabeads™ Untouched™ Mouse T Cells Kit, CellTrace CFSE Cell Proliferation Kit, Foxp3 / Transcription Factor Staining Buffer Set, and SYBR Green qPCR Master Mix were from ThermoFisher Scientific (Waltham, USA). Anti-mouse Phospho-P38 MAPK (cat no.-4511s), P38 MAPK (cat no.-9212s), Phospho-P44/42 MAPK (Erk1/2) (cat no.-4370s), P44/42 MAPK (Erk1/2) (cat no.-4695BC), Phospho-SAPK/JNK (Thr183/Tyr185) (cat no.-4668s), SAPK/JNK (cat no.-9252s), Phospho-STAT3 (Tyr705) (cat no.-9145s), STAT3 (cat no.-9172s), Phospho-STAT1 (cat no.-8826s), STAT1 (cat no.-9172s), Phospho-STAT5 (cat no.-9359s), STAT5 (cat no.-94205s), Phospho-Smad2/3 (cat no.-8828s), Smad2/3 (cat no.-8685s), Phospho-AKT (Thr308) (cat no.-13038T), AKT (cat no.-4691T), Phospho-PI3K (cat no.-17366), PI3K (cat no.-4257), and β-actin (cat no.-8457) antibodies and RIPA buffer

were from Cell Signalling Technology (CST, Danvers, MA, USA). Saponin, Bradford reagent, NP-40, sodium deoxycholate, sodium dodecyl sulphate (SDS), protease inhibitor cocktail, and bovine serum albumin fraction V (BSA) were purchased from Sigma-Aldrich. PVDF membrane and Immobilon Western Chemiluminescent HRP substrate were purchased from Millipore (MA, USA). Sodium chloride and Tris base were purchased from HiMedia. TRIzol reagent was from Invitrogen (MA, USA). PrimeScript 1st strand cDNA Synthesis Kit was from Takara Bio (USA). Primers for Real-time PCR were from GCC Biotech India Pvt Ltd (West Bengal, India). EG00229 trifluoroacetate (an inhibitor for NRP1, cat no.- 6986) was from Tocris (United Kingdom).

Cell culture supernatant collection:

B16-F10 cells were cultured in DMEM following the ATCC protocol (48,49). When the cells reached 60–70% confluence, the culture medium was replaced with a fresh medium. After 24 hours (24h), the cell-free supernatant, or conditioned medium (CM-B16-F10-CS), was collected and stored at −80ºC until further use (50,51).

Trypan blue exclusion test of cell viability:

Purified murine splenic T cells were incubated for 96 hours with varying concentrations of EG with or without TCR activation. After incubation, the cells were harvested and washed with 1X PBS. Trypan blue was added, and the viable cells were manually counted, as described earlier (50). For the positive control, T-cells were either heat-killed (65°C for 5 minutes in a water bath) or exposed to UV light (30 mins) before performing the cell viability assay.

Mice:

Female C57BL/6 mice, aged 6 to 8 weeks, were obtained from the National Institute of Science Education and Research (NISER), Bhubaneswar, for experimentation. The Institutional Animal Ethics Committee (IAEC) approved the study protocols at NISER, adhering to the guidelines established by the Committee for Control and Supervision of Experiments on Animals (CCSEA).

B16-F10 cell injection (subcutaneously or intravenously), EG treatment, tumour volume measurement, metastatic lung nodule count and survivability assay.

Five different groups, each group containing 5 mice, were made. The five groups made were: control, B16-F10 tumour-bearing, EG-treatment in B16-F10 tumour-bearing, B16-F10 intravenously injected and EG-treatment in B16-F10 intravenously injected. B16-F10 cells were injected subcutaneously or intravenously according to the earlier protocol (52). B16-F10 cells in the logarithmic growth phase are harvested with trypsinisation for injection from flasks that were no more than 50% confluent.

Cells were resuspended in ice-cold 1XPBS at a final concentration of $1X10^6$/mL and $4X10^5$/mL cells for subcutaneous and intravenous injections, respectively. For subcutaneous injection, 100µL of cell suspension was injected with an insulin syringe in the upper right flank of mice from both groups while watching for a 'bleb' to form. The same volume of chilled 1XPBS was injected in the control group. For intravenous injection, the tails of mice from both groups and the control group were dipped in warm water until the tail veins were dilated. 0.5mL of cell suspensions were injected with an insulin syringe in the tail veins of mice in B16-F10 intravenously injected and EG-treatment in B16-F10 intravenously injected groups. The same volume of chilled 1XPBS was injected in the control group.

For EG treatment in the B16-F10 tumour-bearing group, EG treatment was given a week to the mice thrice intraperitoneally as described earlier (53,54), (10 mg/kg body weight, 100µL/mouse) starting from the 14th-day post subcutaneous injection after palpable tumours were visible (visible after 10-12 days post-injection) for two weeks. Mice in control and B16-F10 tumour-bearing groups were injected similarly with 1XPBS. Also, from the 14th day, tumour growth progression was periodically measured with a digital calliper (Fisher Scientific), and tumour volumes were calculated using the formula [(tumour length X tumour $width^2$)/2]. After that, mice from all the groups were sacrificed through CO_2 asphyxiation and their spleens were harvested and processed accordingly. The subcutaneous tumours from all the tumour-bearing mice with or without EG treatment were also harvested. For EG treatment in the B16-F10 intravenously injected group, EG treatment was given a week to the mice thrice intraperitoneally as described earlier (53,54) (10 mg/kg body weight, 100µL/mouse) starting from the 2nd-day post intravenous injection for three weeks. Mice in control and B16-F10 intravenously injected groups were injected similarly with 1XPBS. After that, mice from all the groups were sacrificed through CO_2 asphyxiation, cut open and the lungs and heart were pulled out as one unit, ensuring no pulmonary lobes remained in the chest cavity. The lungs were thoroughly rinsed with water and 1XPBS before enumerating metastatic lung nodules. Metastatic lung nodules in mice from all groups were counted on both the lobes of the lungs with a lamp and magnifying glass.

In another batch of mice in B16-F10 tumour-bearing, EG-treatment in B16-F10 tumour-bearing, B16-F10 intravenously injected and EG-treatment in B16-F10 intravenously injected groups, the regimens above for injections and treatments were followed. Still, the mice were not sacrificed, and their survivability rates were evaluated. For subcutaneous survival experiments, mice were killed when tumours reached 20 mm^3 in size or tumour necrosis exceeded 50% of the tumour surface.

T cell isolation, purification, and cell culture:

Around 1.5 million purified murine splenic T cells were cultured in each experimental condition. First, splenocytes from mice were isolated as described elsewhere (55). In brief, spleens from (either control, B16-F10 tumour-bearing or B16-F10 tumour-bearing with EG treatment) C57BL/6 mice were disrupted through a 70 µM cell strainer. RBCs were lysed using RBC lysis buffer, washed with 1X PBS, centrifuged, and resuspended in complete RPMI-1640. T-cells were then purified using the Untouched T cell Isolation Kit according to the manufacturer's protocol (50). Splenocytes were resuspended in an isolation buffer and incubated with biotinylated antibodies. Cells were then washed with excess isolation buffer, centrifuged, and incubated for 15 minutes (mins) with streptavidin-conjugated magnetic beads and then placed in a magnet for 2 mins. The purity of T-cells was ≥ 95%, measured using flow cytometry (BD LSRFortessa™ Cell Analyzer) and analysed by the FlowJo™ v10 software. T cell activation assays were conducted using anti-CD3 (plate-bound) and CD28 antibodies (TCR activation) with or without B16-F10-CS (constituting 5% of the total volume of the cell suspension and media in the experimental setup) and EG00229 trifluoroacetate (EG) at a concentration of 7µM, as previously described. EG concentration of 7 µM in all *in vitro* experimental conditions was used as per earlier studies (41,56) as well as toxicity assay and subsequent estimation of EC_{50} value of EG on purified murine splenic T cells (Supplementary figure S1). The cells were incubated for 96h at 37°C in a humidified CO_2 incubator. For western blot analysis, T cells were cultured with or without B16-F10-CS and EG for 96h and then subjected to TCR activation or left untreated for 15 mins before harvesting.

Flow Cytometry (FC):

Flow cytometric assay was performed as mentioned elsewhere (57,58). Around 1.5 million purified murine splenic T cells were cultured in each experimental condition. In brief, purified T cells from different experimental conditions were suspended in FACS buffer (1X PBS, 1% BSA, 0.01% NaN3) were stained with fluorophore-conjugated antibodies against specific cell surface markers (CD3, CD4, NRP1, NKG2A) in unfixed condition, incubated for 30 min on ice in dark, and washed twice with ice-cold FACS buffer to remove unbound antibodies and suspended in 1% PFA and kept at 4□ for further analysis. Following the manufacturer's protocol, intercellular staining for FOXP3 was done using Foxp3/Transcription Factor Staining Buffer Set. Briefly, purified T cells stained with fluorophore-conjugated anti-mouse CD3 and CD4 antibodies were washed with FACS buffer and incubated with 1X permeabilisation/fixation (perm/fix) buffer for 45mins at room temperature (RT) in the dark. Cells are then washed with 1X permeabilisation (perm) buffer, incubated with anti-mouse fluorophore-conjugated FOXP3 antibody, and incubated for 45 minutes at RT in the dark. Cells were then washed with perm buffer, suspended in 1% PFA and stored at 4□ for further analysis. Intercellular staining of CTLA-4, GATA-3 and T-bet was performed as described elsewhere

(57,58). In brief, purified T cells stained with fluorophore-conjugated anti-mouse CD3 and CD4 antibodies were permeabilized with permeabilization buffer (1X PBS + 0.5% BSA + 0.1% Saponin + 0.01% NaN3) followed by blocking in 1% BSA (in permeabilization buffer) for 30mins at RT in dark. Then, the cells were washed with permeabilization buffer and incubated with anti-mouse fluorophore-conjugated antibodies against respective intercellular markers (CTLA-4, GATA-3 and T-bet) for 30 minutes at RT in the dark. Cells were then washed with permeabilization buffer, suspended in 1% PFA and stored at 4 for further analysis. All the cells were acquired by the BD LSRFortessa™ Cell Analyzer (BD Biosciences) and analysed by the FlowJo™ v10 software (BD Biosciences). The gating strategy was as follows: the $CD3^+$ positive population was selected from the total cell population shown in the FSC vs SSC dot plot. From the $CD3^+$ positive population, the $CD4^+$ cell population was gated (Supplementary figure S5). Within the $CD3^+$ $CD4^+$ dual positive population, the frequency of cells expressing various cellular markers or the expression levels of these markers were measured. The percentage of positive cells expressing the markers was referred to as frequency. In contrast, the expression levels of the markers on cells under different experimental conditions were represented by mean fluorescence intensity (MFI) values. The absolute count of $CD4^+$ $NRP1^+$ Tregs was calculated from the flow cytometric analysis using FlowJo software. Approximately ten thousand cells were acquired per sample.

Apoptosis assay:

Following the manufacturer's protocol, flow cytometry (FC) was performed using the BD Annexin V Detection Kit I to detect apoptotic cells. Briefly, either B16-F10 or NIH-3T3 cells were harvested and washed twice in ice-cold 1XPBS. Cells were then resuspended in 100 µL of 1X Annexin V binding buffer. PE-conjugated Annexin V and 7-AAD cocktail were added to each sample in the appropriate amounts, gently mixed by vortexing, and incubated at room temperature for 15 minutes in the dark. Afterwards, 400 µL of 1X Annexin V binding buffer was added to each tube. The samples were immediately acquired using the BD LSRFortessa™ Cell Analyzer and analysed with FlowJo™ v10 software.

T cell Proliferation Assay:

Purified T cells are incubated with 5 µM CFSE using CellTrace CFSE Cell Proliferation Kit following the manufacturer's protocol, in 1X PBS for 10 minutes at room temperature and then washed three times with RPMI media supplemented with 10% FBS. Then, these CFSE-labelled T cells were cultured in different experimental conditions (Rest, TCR, B16-F10-CS, TCR+B16-F10-CS, TCR+EG and TCR+B16-F10-CS+EG) and incubated in a humified CO_2 incubator for 96h. Also, purified splenic T cells isolated from either control, B16-F10-tumour-bearing or EG-treated B16-F10

tumour-bearing mice were stained with CFSE, washed times with RPMI media supplemented with 10% FBS and incubated in a humified CO_2 incubator for 96h. Around 1.5 million purified murine splenic T cells were cultured in each experimental condition. Post incubation, cells from all experimental conditions were harvested, washed with 1XPBS and stained with fluorophore-conjugated anti-mouse CD3 and CD4 antibodies for 30 mins in the dark at 4□. Cells were then washed with FACS buffer, suspended in 1% PFA and stored at 4□ for further analysis. All the cells were acquired by the BD LSRFortessa™ Cell Analyzer (BD Biosciences) and analysed by the FlowJo™ v10 software (BD Biosciences). The gating strategy was as follows: the $CD3^+$ positive population was selected from the total cell population shown in the FSC vs SSC dot plot. From the $CD3^+$ positive population, the $CD4^+$ cell population was gated. Within the $CD3^+$ $CD4^+$ dual positive population, the MFI of CFSE-stained cells was calculated.

***In vitro* suppression assay of Tregs:**

The immunosuppressive potential of Tregs was evaluated through an *in vitro* suppression assay (37). Purified splenic T cells from control, B16-F10 tumour-bearing, or B16-F10 tumour-bearing with EG treatment C57BL/6 mice were cultured with or without TCR, B16-F10-CS, or EG treatment for 96 hours in a humidified CO_2 incubator. Around 1.5 million purified murine splenic T cells were cultured in each experimental condition. Forty-eight hours before the end of this incubation, about 10 million purified splenic T cells from normal C57BL/6 mice were treated with anti-CD3 (plate-bound) and CD28 antibodies for TCR activation and incubated for 36-48 hours. These TCR-activated T cells were then stained with CFSE. They were co-cultured with the previously prepared T cells under various conditions (Rest, TCR, B16-F10-CS, TCR+B16-F10-CS, TCR+EG, and TCR+B16-F10-CS+EG) or with T cells from control and tumour-bearing mice with or without EG treatment in a 1:1 ratio, at a total cell density of 1.5 million cells/mL, for 96 hours. After incubation, all cells were harvested, washed with PBS, and stained with fluorophore-conjugated anti-mouse CD3 and CD4 antibodies for 30 minutes in the dark at 4°C. The cells were then washed, suspended in 1% PFA, and stored at 4°C for further analysis. The cells were acquired using a BD LSRFortessa™ Cell Analyzer and analysed with FlowJo™ v10 software. The gating strategy involved selecting the $CD3^+$ population from the total cell population in the FSC vs. SSC dot plot and then gating the CD4+ population from the $CD3^+$ cells. Within the $CD3^+$ $CD4^+$ population, the MFI of CFSE-stained cells was calculated. The proliferation rate of CFSE-labelled TCR-activated effector T cells in the presence of cells from control or different experimental conditions or tumour-bearing mice with or without EG treatment was then determined.

BD Cytometric Bead Array

To quantify secreted cytokine levels in purified T cells isolated from control, B16-F10 tumour-bearing, or B16-F10 tumour-bearing with EG treatment C57BL/6 mice, the cells were cultured with or without TCR, B16-F10-CS, or EG treatment for 96 hours in a humidified CO_2 incubator. Around 1.5 million purified murine splenic T cells were cultured in each experimental condition. The BD Cytometric Bead Array (CBA) Mouse Th1/Th2/Th17 Cytokine Kit was used per the manufacturer's protocol (59). A vial of lyophilized standards was opened, transferred to a 15 mL conical polypropylene tube labelled "Top Standard," and reconstituted with 2.0 mL of Assay Diluent. The mixture was gently pipetted after equilibrating at room temperature for 15 minutes. A series of 1.5 mL tubes were labelled (1:2, 1:4, 1:8, 1:16, 1:32, 1:64, 1:128, 1:256) and filled with 300 µL of Assay Diluent each. Serial dilutions were performed, starting with 300 µL from the Top Standard and continuing sequentially. A tube with only Assay Diluent was the 0 pg/mL negative control. The required number of assay tubes was determined, and each Capture Bead suspension was vortexed before mixing. A 10 µL aliquot of each Capture Bead per assay tube was combined in a tube labelled "mixed Capture Beads," vortexed, and 50 µL was added to all assay tubes. Then, 50 µL of Mouse Th1/Th2/Th17 Cytokine Standard dilutions were added to control tubes, and 50 µL of each unknown sample was added to labelled sample tubes. Subsequently, 50 µL of the Mouse Th1/Th2/Th17 PE Detection Reagent was added to all assay tubes. Tubes were incubated for 2 hours at room temperature and protected from light. Post incubation, 1 mL of Wash Buffer was added to each tube, centrifuged at 200g for 5 minutes, and the supernatant was discarded. Finally, 300 µL of Wash Buffer was added to resuspend the bead pellet. Samples were immediately analysed using the BD LSRFortessa™ Cell Analyzer and FlowJo™ v10 software, following the manufacturer's protocols (59).

Western Blot Analysis:

Protein expression was assessed by western blot analysis following previously described protocols (57). Purified T cells from control, B16-F10 tumour-bearing, or B16-F10 tumour-bearing with EG treatment C57BL/6 mice were cultured with or without TCR, B16-F10-CS, or EG treatment for 96 hours in a humidified CO_2 incubator. Around 10 million purified murine splenic T cells were cultured in each experimental condition. After incubation, cells were washed with ice-cold PBS, and whole cell lysate (WCL) was prepared using RIPA lysis buffer (150 mM NaCl, 1% NP-40, 0.5% sodium deoxycholate, 0.1% SDS, 50 mM Tris, pH 8.0, with protease inhibitors) and centrifuged at 13,000 rcf for 30 minutes at 4 °C. Protein concentration was determined using the Bradford assay. Equal amounts of protein were mixed with 6X Laemmli buffer, loaded onto 10% SDS-PAGE gels, and transferred to PVDF membranes. Membranes were blocked with 3% BSA in TBST and incubated overnight with various anti-mouse primary antibodies (diluted 1:1000 in blocking buffer) targeting

Phospho-P38 MAPK, P38 MAPK, Phospho-P44/42 MAPK (Erk1/2), P44/42 MAPK (Erk1/2), Phospho-SAPK/JNK (Thr183/Tyr185), SAPK/JNK, Phospho-STAT3 (Tyr705), STAT3, Phospho-STAT1, STAT1, Phospho-STAT5, STAT5, Phospho-Smad2/3, Smad2/3, Phospho-AKT (Thr308), AKT, Phospho-PI3K, PI3K, and β-actin. After thorough washing with TBST, membranes were incubated with HRP-conjugated anti-mouse or anti-rabbit secondary antibodies (diluted 1:4000 in blocking buffer) for 2 hours at room temperature. Membranes were washed again with TBST and subjected to chemiluminescence detection using Immobilon Western Chemiluminescent HRP substrate (Millipore). They were imaged with Bio-Rad Gel Doc and Image Lab software while normalising to the corresponding loading control. The expression of β-actin in all samples was quantified for sample loading control.

2.13 cBioPortal analysis:

The potential alterations of the NRP1 gene in previously reported cancer patient databases were analysed using the online server cBioPortal (https://www.cbioportal.org/, accessed on 6 June 2024). cBioPortal analysis was done in 212 melanoma cancer patients from a combined analysis of three studies: Metastatic Melanoma (DFCI, Science 2015), Melanoma (MSK, NEJM 2014), and Metastatic Melanoma (UCLA, Cell 2016) (Figure 2A). Additionally, 2683 cancer patient samples from a Pan-cancer study of whole genomes (ICGC/TCGA, Nature 2020) were also evaluated in the cBioPortal.

Statistical analysis:

Statistical Analysis was performed using the GraphPad Prism 8.0 software (GraphPad Software Inc., San Diego, CA, USA). Data are represented as Mean ± SEM. Unless otherwise mentioned, the comparison between the groups was performed by the One-way ANOVA or Student's t-test. To estimate the EC_{50} value of EG on purified murine splenic T cells, EC_{50} shift from a non-linear dose vs response XY plot (where X is concentration) was calculated using GraphPad Prism. One column T and Wilcoxon test was performed using GraphPad Prism to determine the statistical significance of fold change in gene expression between tumorigenic and non-tumorigenic cells. The statistical significance between the Kaplan–Meier survivability graphs of C57BL/6 mice injected with B16-F10 cells subcutaneously or intravenously with or without EG treatment was evaluated through the Log Rank test using GraphPad Prism. The data presented here are representative of at least three independent experiments. $P < 0.05$ is considered a statistically significant difference between the groups.

Results

Elevation of regulatory T cells (Tregs) frequency in murine splenic population during B16-F10 cell culture supernatant (B16-F10-CS) treatment, *in vitro.*

The predominance of intratumoral Tregs and their role in immunosuppression, cancer progression, metastasis, and poor patient survival outcomes has been extensively reported (9,10,60). It has also been noted that cancer cell-conditioned media (CM) induces the generation of Tregs *in vitro*, facilitating cancer-mediated immunosuppression (61,62). Furthermore, B16-F10 cell culture supernatant (B16-F10-CS) has been reported to induce immunosuppression in murine T cells (50,63). Accordingly, the current study assessed the possible increase in peripheral Tregs in the murine splenic T cell population in vitro during B16-F10-CS treatment (**Figure 1**).

Flow cytometric dot plots revealed that the frequency of FOXP3, NKG2A, and NRP1 positive T cells increased in TCR+B16-F10-CS-treated condition compared to resting, only TCR-activated, and only B16-F10-CS-treated conditions (**Figure 1A**) indicating an increase of suppressor T cell population in immunosuppressive B16-F10-CS-treated condition. While no discernible change in the frequency of FOXP3-expressing T cells was observed between resting and B16-F10-CS-treated T cells (**Figure 1B**), the frequency of NKG2A and NRP1 positive T cells was elevated in B16-F10-CS-treated conditions compared to the resting T cells (**Figures 1C and D**). Although the possible alteration in frequency of other Treg populations such as CTLA-4, PD-1, PD-L1, and positive populations was evaluated, no discernible change was observed when compared between *in vitro* experimental conditions with TCR and TCR+B16-F10-CS treatment (**Supplementary figure S2**). Thus, the frequency of FOXP3, NKG2A, and NRP1 positive suppressor T cells was elevated upon immunosuppressive B16-F10-CS treatment in TCR-activated T cells, *in vitro*.

cBioPortal and mRNA analysis showed increased Neuropillin-1 (NRP1) expression in melanoma patients and cell lines, respectively, and its inhibition triggered apoptosis in tumorigenic B16-F10 cells.

In our previous data, the frequency of FOXP3, NKG2A and NRP1 positive suppressor T cells was elevated during immunosuppressive B16-F10-CS treatment. NRP1 is reported to be the stability and functionality marker for regulatory suppressor T cells, and its depletion has been reported to alleviate Treg suppressive activity (26). It has also been previously reported that carcinoma cell lines, including melanoma, depend on NRP1 for viability and proliferation by stimulating multiple growth factor receptors (44,47,64). Further, NRP1 expression in tumour-associated vessels and various cancers is correlated with tumour progression, tumour aggressiveness, advanced stages, and poor prognosis, particularly in melanoma and breast cancer (23,47,65). Accordingly, the expression of NRP1 in cancer patients, including those with melanoma, was analysed using cBioPortal. At the

same time, qRT-PCR-based mRNA quantification of the NRP1 gene was done in tumorigenic B16-F10 and non-tumorigenic NIH-3T3 cell lines. The potential apoptotic effect of NRP1 inhibition on B16-F10 and NIH-3T3 cell lines was also evaluated. (**Figure 2**).

The potential alterations of the NRP1 gene in previously reported cancer patient databases were analysed using the online server cBioPortal (https://www.cbioportal.org/, accessed on 6 June 2024). Oncoprint from cBioPortal revealed that the copy number alterations (CNA) of the NRP1 gene were observed to be in 10 per cent of 212 melanoma cancer patients, based on a combined analysis of three studies: Metastatic Melanoma (DFCI, Science 2015), Melanoma (MSK, NEJM 2014), and Metastatic Melanoma (UCLA, Cell 2016) (**Figure 2A**). Additionally, as depicted in the monoprint, approximately 4 per cent CNA of the NRP1 gene was identified among 2683 cancer patient samples from a Pan-cancer study of whole genomes (ICGC/TCGA, Nature 2020). Among the various mutation types, amplification of the NRP1 gene was observed in both melanoma and other cancer patients with CNA. Furthermore, the plotted bar graph depicted that among all other cancer patients, the frequency of alteration of the NRP1 gene was highest in melanoma cancer patients based on the CNA and mutation load data from the Pan-cancer mentioned above (**Figure 2B**).

To validate the cBioPortal findings indicating an increased expression of the NRP1 gene in melanoma and other cancer patients, mRNA levels of NRP1 were compared between tumorigenic (B16-F10) and non-tumorigenic (NIH-3T3) cells. NRP1 expression was elevated in B16-F10 cells compared to NIH-3T3 cells (**Figure 2C**).

Since NRP1 has been reported to be significantly involved in melanoma cell viability and proliferation (23,65), the effect of NRP1 inhibition in B16-F10 and NIH-3T3 cells with specific small molecule inhibitor EG00229 trifluoroacetate (EG) was evaluated with Annexin V and 7-AAD dual staining. Flow cytometric dot plots and representative bar graphs showed insignificant necrotic cell death (indicated by only 7-AAD positive cells) in both B16-F10 and NIH-3T3 cells upon treatment with varied concentrations of EG (Figure 2D, Supplementary Figure **S3**). However, a gradual increase of apoptotic B16-F10 cells (both early and late) was observed upon treatment with EG at higher doses than 10μM. Negligible cell death was observed in NIH-3T3 cells treated with EG. Thus, cBioPortal analysis revealed that NRP1 expression was elevated in cancer patients, including melanoma. Furthermore, mRNA quantification studies revealed that NRP1 expression was heightened in B16-F10 melanoma cell lines compared to the control cell line. Additionally, NRP1 inhibition induced apoptosis in tumorigenic B16-F10 cells but not in non-tumorigenic NIH-3T3 cells.

Inhibition of Neuropillin-1 (NRP1) alleviated expression of regulatory T cell (Treg) markers in splenic T cells treated with B16-F10 cell culture supernatant (B16-F10-CS) *in vitro*.

There is a significant interest in identifying pathways that control Treg stability, as many immune-mediated diseases involve excessive or limited Treg function (66). Previous studies have identified that the NRP1 pathway is crucial for intratumoral Treg stability but unnecessary for maintaining immune homeostasis. This led to a possible suggestion that modulating the NRP1 pathway by blocking Sema4A with antibodies or soluble antagonists could be a viable strategy to limit tumour-induced tolerance without triggering autoimmunity (26). Furthermore, earlier reports also suggest that, while NRP1-deficient Tregs maintained FOXP3 expression (67,68), T cell-specific ablation of NRP1 expression led to a notable reduction in the number of tumour-infiltrating FOXP3+ Tregs (69). It has also been reported that even though NRP1 expression has been observed in natural killer T (NKT) cells newly emigrated from the thymus, there is minimal information on the role of NRP1 in NKT cells (70). Furthermore, although numerous studies show the elevated expression of these markers in intratumoral Tregs (37,69,71), research on the expression and regulatory role of peripheral Tregs in cancerous environments is limited. Accordingly, the expression of T cell immunosuppressive markers (NRP1, FOXP3 and NKG2A) on TCR-activated B16-F10-CS-treated $CD4^+$ splenic T cells, with or without NRP1 inhibition with EG, was evaluated (**Figure 3**).

It was observed that the expression of immunosuppressive Treg markers (NRP1, NKG2A and FOXP3) commonly known as inhibitory receptors (IRs) was elevated in splenic T cells cultured in TCR+B16-F10-CS condition. These IRs' expression was reduced upon EG treatment (**Figure 3A-D**). Similarly, the elevated expression of these IRs in only TCR-activated splenic T cells was alleviated upon EG treatment. Although the possible alteration in expression of other Treg markers, such as CTLA-4, PD-1, and PD-L1, was evaluated, no discernible change was observed when compared between *in vitro* experimental conditions with TCR and TCR+B16-F10-CS treatment (**Supplementary figure S4**). Thus, it was observed that NRP1 inhibition with EG in $CD4^+$ splenic T cells cultured in immunosuppressive B16-F10-CS not only reduced NRP1 expression but also decreased NKG2A and FOXP3 expression *in vitro*.

Inhibition of Neuropilin-1 (NRP1) enhanced proinflammatory cytokine secretion and T cell proliferation while decreasing Treg suppressive activity and the release of immunosuppressive cytokines in splenic T cells treated with B16-F10 cell culture supernatant (B16-F10-CS), *in vitro*.

It has been reported earlier that NRP1 acts as a functionality and stability marker for Treg, and its depletion diminished Treg immunosuppressive potential, promoted Treg fragility and ameliorated anti-tumour response (7,23,31,72–74). Our previous data showed that NRP1 inhibition downregulated the expression of NRP1 and other IRs in B16-F10-CS-treated splenic T cells,

indicating its probable role in immune modulation. Accordingly, the immunosuppressive potential of CD4+ splenic T cells treated with B16-F10-CS, with or without TCR activation and NRP1 inhibition with EG, was evaluated (**Figure 4**).

CBA analysis for quantification of secreted cytokines in TCR+B16-F10-CS-treated splenic T cells revealed that effector cytokines (TNF, IFN-γ, IL-2, IL-6) (**Figure 4A, B, D and F**) and immunomodulatory cytokines (IL-10, IL-17A) (**Figure 4C and E)** secretions were attenuated and augmented, respectively. This was reversed in TCR+B16-F10-CS+EG-treated splenic T cells. There was no significant change in TNF, IFN-γ, and IL-17A levels in only TCR-activated T cells with or without EG treatment. However, levels of IL-2 and IL-6 were increased, while IL-10 levels were decreased in TCR+EG-treated T cells compared to untreated TCR-activated ones.

Furthermore, the flow cytometric histogram from the CFSE assay and representative bar diagram depicted that cell proliferation was diminished in TCR+B16-F10-CS-treated splenic T cells. This reduced proliferative rate was ameliorated in TCR+B16-F10-CS+EG-treated splenic T cells (**Figure 4G and Supplementary figure S7A**). There was no discernible change in cell proliferation of TCR-activated T cells with or without EG treatment. Furthermore, the absolute $CD4^+$ $NRP1^+$ Treg count among 1.5 million purified murine splenic T cells cultured in different experimental conditions was evaluated (**Supplementary figure S6A and B**). It was found that the absolute count of $CD4^+$ $NRP1^+$ Tregs among 1.5 million purified murine splenic T cells cultured in different experimental conditions was increased in the TCR+B16-F10-CS condition as compared to only the TCR-activated condition. NRP1 inhibition with EG showed diminished $CD4^+$ $NRP1^+$ Treg number compared to TCR and TCR+EG or TCR+B16-F10-CS and TCR+B16-F10-CS+EG conditions.

Moreover, the immunosuppressive potential of CD4+ TCR-activated splenic T cells with or without B16-F10-CS and EG treatment was evaluated by assessing the cell proliferation of CFSE labelled co-cultured TCR-activated effector T cells. It was observed that TCR+B16-F10-CS+EG treated CD4+ T cells increased the proliferation of co-cultured effector T cells concerning only TCR+B16-F10-CS-treated T cells (**Figure 4H and Supplementary figure S7B**).

Thus, it was observed that NRP1 inhibition with EG not only upregulated CD4+ T cell proliferation and effector cytokine response in TCR-activated B16-F10-CS-treated T cells but also downregulated secretion of immunomodulatory cytokines and Treg suppressive activity.

Inhibition of Neuropilin-1 (NRP1) alleviated the STAT, Smad2/3, and ERK-MAPK pathways while enhancing the AKT/PI3K pathway in splenic T cells treated with B16-F10 cell culture supernatant (B16-F10-CS), *in vitro*.

NRP1 in cancer cells and intratumoral Tregs is reported to regulate STAT, PI3K/AKT, TGF-β-mediated Smad2/3, and ERK MAPK signalling pathways during various cancers, thereby facilitating cancer progression and metastasis (34,75–80). Accordingly, the effect of NRP1 inhibition with EG on STAT, PI3K/AKT, TGF-β-mediated Smad2/3, and ERK-MAPK signalling in murine splenic T cells cultured in immunosuppressive B16-F10-CS was evaluated (**Figure 5**).

Western blot analysis and representative bar graphs revealed that TCR+B16-F10-CS+EG-treated splenic T cells exhibited a diminished expression of phosphorylated STAT1, STAT3, STAT5, Smad2/3, and ERK as compared to TCR+B16-F10-CS-treated ones (**Figure 5A, B, C, D, E and H**). Conversely, TCR+B16-F10-CS+EG-treated T cells showed increased phosphorylated AKT and PI3K expression compared to only TCR+B16-F10-CS-treated ones (**Figure 5F and G**). No discernible alteration in phosphorylated STAT5 and AKT expression was observed in TCR-activated murine splenic T cells with or without NRP1 inhibition. However, the expression of phosphorylated STAT1, STAT3, Smad2/3, and ERK was reduced in TCR+EG-treated splenic T cells compared to only TCR-activated ones. On the contrary, PI3K phosphorylation was upregulated in TCR+EG-treated splenic T cells compared to only TCR-activated ones. No visible alteration in the expression of phosphorylated SAPK/JNK and P38 (**Figure 5A and Supplementary Figure S8**) was observed when compared between TCR-activated and TCR+EG-treated T cells or TCR+B16-F10-CS-treated and TCR+B16-F10-CS+EG treated T cells. This indicated that NRP1 might not directly regulate SAPK/JNK and P38 MAPK pathways in splenic T cells.

Therefore, it was observed that NRP1 inhibition with EG attenuated STAT, Smad2/3 and ERK MAPK phosphorylation while augmenting AKT and PI3K phosphorylation in TCR-activated splenic T cells treated with B16-F10-CS.

Expression of regulatory T cell (Treg), Th_1 and Th_2 markers was attenuated in splenic T cells isolated from B16-F10 subcutaneous tumour bearing mice treated with Neuropillin-1 (NRP1) inhibitor.

It has been reported that expression of IRs such as NRP1, NKG2A, FOXP3, PD-1, PD-L1, CTLA-4, GATA-3 and T-bet in intratumoral Tregs plays a crucial role in the tumour microenvironment and regulated tumour cell survival, proliferation, metastasis and patient outcome and thereby are targets for anti-cancer immunotherapy (71,79,81–84). Conversely, studies delineating the expression of these IRs in peripheral Tregs and their possible role in tumour progression and metastasis are limited (72,85). Furthermore, although inhibition/depletion of NRP1 is known to regulate FOXP3, T-bet, CTLA-4 and PD-1 expression and function in intratumoral Tregs (23), its possible role in modulation of these IRs in peripheral Tregs during cancer is unclear. Accordingly, expression of IRs such as

NRP1, NKG2A, FOXP3, PD-1, PD-L1, CTLA-4, GATA-3 and T-bet in murine splenic T cells isolated from B16-F10 melanoma tumour-bearing mice with or without NRP1 inhibitor (EG) treatment, was evaluated.

It was observed that splenic T cells isolated from B16-F10 melanoma tumour-bearing mice with EG treatment showed attenuation in the expression of Treg markers such as NRP1, NKG2A, FOXP3, PD-1, PD-L1 and CTLA-4, but also Th_2 marker GATA-3 when compared to T cells isolated from untreated tumour bearing mice (**Figure 6A-G and Supplementary figure S9A-G**). Conversely, T-bet (Th_1) expression was augmented in splenic T cells isolated from EG-treated tumour-bearing mice as compared to T cells isolated from untreated tumour-bearing mice (**Figure 6H and Supplementary figure S9H**).

Thus, it was observed that NRP1 inhibition with EG in subcutaneous B16-F10 melanoma tumour-bearing mice reduced the expression of IR molecules like NRP1, NKG2A, FOXP3, CTLA-4, PD-1, PD-L1 and Th_2 cell differentiation transcription factor GATA-3 and elevated Th_1 cell differentiation transcription factor T-bet in murine peripheral splenic Tregs.

Increase in proliferation and reduction in suppressive activity of Tregs of purified splenic T cells isolated from B16-F10 subcutaneous tumour-bearing mice treated with Neuropilin-1 (NRP1) inhibitor.

NRP1 is reported to negatively regulate the proliferation of $CD4^+FOXP3^+$ Tregs (7). Additionally, it has been reported that NRP1 inhibits the suppressive function of intratumoral regulatory T cells by reducing their proliferation (37) NRP1 depletion has been shown to attenuate the proliferation of $CD4^+$ effector T cells and promote transplantation tolerance in graft-versus-host disease (GVHD) (86). Accordingly, the proliferation of $CD4^+$ splenic T cells isolated from B16-F10 subcutaneous tumour-bearing mice, with or without EG treatment, and their suppressive activity on the TCR-activated splenic effector T cells were evaluated by the CFSE cell proliferation assay (**Figure 7**).

It was observed that TCR-activated splenic T cells isolated from EG-treated B16-F10 tumour-bearing mice exhibited increased proliferation compared to those isolated from untreated tumour-bearing mice (**Figure 7A and Supplementary figure S10A**). Furthermore, the absolute $CD4^+$ $NRP1^+$ Treg counts in murine spleens isolated from count control, untreated tumour-bearing and EG-treated tumour-bearing C57BL/6 mice were evaluated (**Supplementary figure S6A and C**). It was found that the absolute count of $CD4^+$ $NRP1^+$ Tregs isolated from untreated tumour-bearing mice spleens was alleviated compared to EG-treated tumour-bearing mice.

Similarly, to evaluate the possible regulation of the suppressive activity of the aforementioned T cells, TCR-activated effector T cells were co-cultured with splenic T cells from EG-treated B16-F10 tumour-bearing mice. $CD4^+$ splenic T cells isolated from EG-treated tumour-bearing mice showed lesser suppression of co-cultured effector T cell proliferation as compared to $CD4^+$ splenic T cells isolated from untreated tumour-bearing mice (**Figure 7B and Supplementary figure S10B**).

Thus, EG treatment in B16-F10 tumour-bearing mice increased the proliferation of splenic T cells and reduced their immunosuppressive potential compared to T cells from untreated mice.

Neuropillin-1 (NRP1) inhibitor treatment ameliorated B16-F10 lung metastasis, reduced subcutaneous tumour volume, and increased the survivability of C57BL/6 mice.

NRP1 depletion, knockout and inhibition with inhibitors, monoclonal antibodies and nanobodies have shown remarkable anti-cancerous effects and have been reported to have attenuated angiogenesis, tumorigenesis, tumour growth and metastasis and improved survivability (7,23,29–37,73). While various inhibitors and microRNAs have shown anti-cancer activity by inhibiting NRP1, EG00229 has been reported to be the most specific and characteristic inhibitor of NRP1's interaction with VEGFA (28). It reportedly shows significant tumour-suppressive effects in cancers (38,39,87–89). Furthermore, even though NRP1 has been reported as a potential target for melanoma and repurposed drugs have reportedly shown significant anti-tumour activity against melanoma (45,46), any possible anti-tumour activity of EG00229 on melanoma is yet to be studied. Accordingly, the potential of the NRP1 inhibitor EG00229 trifluoroacetate (EG) in reducing the tumour growth and lung metastasis of B16-F10 melanoma tumour and improving survival rates in C57BL/6 mice were evaluated.

Mice treated with EG showed fewer metastatic lung nodules from intravenous injection of B16-F10 melanoma cells than untreated mice (**Figure 8A and D**). Additionally, less subcutaneous tumour growth was observed in tumour-bearing mice treated with EG than in untreated mice (**Figure 8B and F and Supplementary Figure S11**). According to log-rank P analysis, EG treatment improved survival rates in mice injected with B16-F10 cells subcutaneously or intravenously (**Figure 8C and E**).

Thus, treatment with EG reduced B16-F10 metastasis and tumour growth and improved the survivability rate in C57BL/6 mice.

Discussion

A GLOBOCAN study identified melanoma as the deadliest skin cancer, posing a significant threat to public health and economic burden. Despite being preventable, melanoma is severe due to its high

metastasis risk (90). Studies indicated that melanoma is immunogenic with a poor prognosis under immunosuppressive conditions, involving mechanisms like surface antigen down-regulation, mutations, lack of costimulatory function, secretion of immunosuppressive cytokines, and tolerance induction. Melanomas are also reported to recruit regulatory immune cells, inhibiting effector T-cell function and expressing molecules that inhibit activated immune cells (2). These studies led to the development of ICIs targeting PD-1/PD-L1 and CTLA-4, revolutionising cancer immunotherapy, especially against melanoma. Building on their success, new antibodies targeting LAG-3, TIM-3, VISTA, BRAF, mitogen-activated extracellular signal-regulated kinase (MEK), and T-cell immunoreceptor with Ig and ITIM domains (TIGIT) are currently in clinical trials alone or with anti-CTLA-4 and anti-PD-1/PD-L1. The success of these ICIs in melanoma confirmed their therapeutic impact. However, even with combination ICIs, about half of patients do not experience long-lasting benefits (21). IrAEs are also common, particularly with combination ICI therapy. Therefore, identifying molecular markers that regulate immune checkpoints and developing suitable immunotherapeutic regimens is crucial (11,23). Recently, NRP1 has been identified as a potential therapeutic target for cancer immunotherapy. NRP1 is reported to be upregulated in several cancers, promoting progression and poor prognosis (23,25,28,31,47,91). Inhibition or depletion of NRP1 has been shown to reduce angiogenesis and tumour progression and enhance other immunotherapies. Although various inhibitors, monoclonal antibodies, and nanobodies target NRP1, EG00229 is the most specific inhibitor identified (7,27,32,37,65,92,93). Additionally, NRP1 depletion and inhibition have been shown to reduce the prevalence and immunosuppressive potential of intratumoral Tregs (94). While EG00229's anti-cancer potential has been demonstrated in different cancers, its role in melanoma and regulation of Tregs remains unknown. Accordingly, the potential immunotherapeutic role of EG00229 trifluoroacetate (EG) in regulating splenic peripheral Tregs during B16-F10 melanoma-driven immunosuppression was investigated. Also, its possible anti-tumorigenic effects in reducing B16-F10 tumour growth and metastasis and improving survival were evaluated.

Although several studies have shown the infiltration of immunoregulatory T cells, such as FOXP3+, NRP1+, and NKG2A+ Tregs, in the intratumoral region and their prevalence in different cancer patients leading to poor prognosis (9,10,60), their presence in peripheral sites during cancer-mediated immunosuppression has not been extensively studied. Additionally, while earlier reports have described B16-F10 melanoma tumour-mediated and B16-F10 cancer cell conditioned media (B16-F10-CS)-induced immunosuppression (50,63), the potential upregulation of Tregs during *in vitro*, B16-F10-CS-mediated immunosuppression has not yet been explored. It was observed that the frequency of FOXP3, NKG2A, and NRP1 positive Treg populations increased in TCR-activated B16-F10-CS-treated peripheral splenic T cells compared to TCR-activated T cells alone (**Figure 1**).

Meanwhile, upregulation of NKG2A and FOXP3 positive peripheral Tregs has been reported with head and neck squamous cell carcinoma (HNSCC) and gastric cancer (GC) cell conditioned media (61,62), respectively; the upregulation of $NRP1^+$, $NKG2A^+$, and $FOXP3^+$ peripheral splenic Tregs in the presence of B16-F10 CM was observed for the first time. Additionally, NRP1+ and NKG2A+ Tregs were upregulated only in B16-F10-CS-treated conditions compared to resting conditions (**Figure 1A, C and D**), while FOXP3+ Tregs remained comparable in both conditions, highlighting the importance of TCR-dependent FOXP3 upregulation, as reported earlier (95) (**Figure 1A and B**).

Furthermore, NRP1 is reported to be upregulated in various cancers and is essential for tumour cell survival, proliferation, and metastasis (23,25,26,31,44,92,96). Similarly, oncoprint from cBioPortal analysis of patient data from a pan-cancer study (ICGC/TCGA, Nature 2020) and a combined study of melanoma patients (Metastatic Melanoma (DFCI, Science 2015), Melanoma (MSK, NEJM 2014), and Metastatic Melanoma (UCLA, Cell 2016)) depicted that NRP1 gene expression was amplified in all cancer patients including melanoma (**Figure 2A**). Interestingly, it was observed from the oncoprint and the bar graph from cBioPortal analysis that the alteration frequency of the NRP1 gene was higher among melanoma cancer patients, suggesting NRP1 is a suitable therapeutic target for melanoma cancer as reported elsewhere (**Figure 2A and B**). Additionally, mRNA quantification showed elevated NRP1 gene expression in tumorigenic B16-F10 cells compared to non-tumorigenic NIH-3T3 cells (**Figure 2C**). Moreover, NRP1 was crucial for B16-F10 cell survival, as inhibition of NRP1 with EG induced apoptosis in B16-F10 cells at doses higher than 10 μM, but did not affect NIH-3T3 cells at the same dose (**Figure 2D, Supplementary figure S3**). The current findings validated earlier findings that NRP1 was indispensable for cancer cell survival and proliferation (23,65).

Earlier reports suggested that NRP1 is essential for both cancer cells and the stability and functioning of Tregs (26,66,91). Other NRP1 inhibitors have been shown to reduce the immunosuppressive potential of intratumoral Tregs (37). Although the NRP1 inhibitor EG is known for its anti-tumour activity in various cancers (41,47), its potential role in Tregs has remained unexplored until now. To the best of our knowledge, this study is the first to highlight the possible regulatory role of EG on peripheral Tregs. The findings revealed that NRP1 inhibition with EG in peripheral Tregs cultured in B16-F10-CS, *in vitro*, not only reduced their NRP1 expression but also decreased the expression of other immunosuppressive markers like NKG2A and FOXP3 (**Figure 3**), signifying the regulatory role of NRP1 in peripheral Tregs.

NRP1 inhibition also augmented T-cell effector responses in several cancers and facilitated anti-tumour responses (23,26). The current study studied the possible regulatory role of EG-mediated

NRP1 inhibition in peripheral Tregs cultured in B16-F10-CS *in vitro*. It was found that the EG-mediated NRP1 inhibition in TCR+B16-F10-CS-treated T cells not only led to their increment in effector cytokine secretion but also decreased their immunoregulatory cytokine secretion that is known to facilitate Treg-mediated immunosuppression otherwise (20,97) (**Figure 4A-F**). Although IL-17A has been reported to be an inflammatory cytokine, it has also been studied to promote Treg-mediated immunosuppression (98,99). In the current study, it has been observed that EG-mediated NRP1 inhibition in TCR+B16-F10-CS-treated splenic T cells downregulated their IL-17A secretion as compared to only TCR+B16-F10-CS treated ones, highlighting the role of NRP1 in IL-17A secretion and regulatory role in peripheral Tregs for the first time. NRP1 has also been reported to diminish $CD4^+$ $FOXP3^+$ Treg and $CD4^+$ effector T cell proliferation in GVHD and metastatic melanoma patients, respectively (100). Similarly, TCR+B16-F10-CS+EG-treated $CD4^+$ T cells also showed augmented proliferation compared to only TCR+B16-F10-CS-treated ones, which validated previous findings (**Figure 4G and Supplementary figure S7A**). NRP1 expression on Tregs is also known to enhance its immunosuppressive potential. Tregs facilitate immunosuppression during cancer by ameliorating effector T cell proliferation (101,102). In the current study, it was observed that TCR+B16-F10-CS+EG-treated peripheral splenic T cells augmented the proliferation of TCR-activated CFSE-labelled $CD4^+$ effector T cells, thus highlighting that EG-mediated inhibition diminishes the immunosuppressive potential of peripheral Tregs, *in vitro* (**Figure 4H and Supplementary figure S7B**). It was also observed that TCR, B16-F10-CS and EG treatment did not alter the percentage of $CD4^+$ T cells in each experimental condition (**Supplementary figure S5A and B**). However, the absolute number of $CD4^+$ $NRP1^+$ Tregs decreased upon EG treatment in TCR and TCR+B16-F10-CS conditions compared to untreated TCR and TCR+B16-F10-CS conditions. This decrease in $CD4^+$ $NRP1^+$ Tregs in EG-treated conditions might have contributed to their diminished immunosuppressive potential observed here (**Figure 4H and Supplementary figure S7B**).

NRP1 is reported to be a receptor for both Sema3a and VEGF. During cancer, NRP1 on Tregs facilitated immunosuppression by helping Tregs gather through VEGF co-receptor activity and maintaining their stability through Sema4a binding. This process promoted Treg survival and function by regulating the Akt-mTOR signalling and the PTEN-Akt-FoxO pathway. (24–26). It has been reported that Akt and PI3K phosphorylation is diminished during cancer conditions, and phosphorylated PTEN-mediated FOXP3 expression in Tregs is promoted (103). Accordingly, it was found that EG-mediated NRP1 inhibition in TCR+B16-F10-CS-treated peripheral Tregs showed elevated expression of phospho-Akt and PI3K as compared to only TCR+B16-F10-CS treated ones (**Figure 5A, F and G**). In addition, FOXP3 expression was also diminished in TCR+B16-F10-

CS+EG-treated peripheral splenic T cells, thus validating previous findings (**Figure 2A and D**). Furthermore, it has also been reported that NRP1 on Tregs upregulated Smad2/3, ERK and P38 pathways through TGF-β and IL-10 mediated VEGFR and EGFR signalling (102,104). SAPK/JNK signalling is also reported to be downregulated in non-small-cell lung cancer cells (NSCLCC) through VEGFR signalling (105). Accordingly, it was found that EG-mediated NRP1 inhibition in TCR+B16-F10-CS-treated peripheral splenic T cells downregulated the expression of phospho-Smad2/3 and ERK as compared to only TCR+B16-F10-CS-treated ones (**Figure 5A, E and H**). However, no change in phosphorylated levels of P38 and SAPK/JNK was observed when compared between TCR+B16-F10-CS treated peripheral splenic T cells with or without EG treatment (**Figure 5A and Supplementary figure S8**). This indicates that NRP1 might not have a significant role in regulating SAPK/JNK and P38 signalling in T cells, but further experimentations on NRP1 inhibited/depleted B16-F10 and TILs isolated from B16-F10 tumour must be conducted to validate this hypothesis. Moreover, while the significance of STAT signalling in different cancers and regulation of NRP1-mediated immunosuppression of Tregs through STAT signalling has been extensively studied, the regulatory role of NRP1 in STAT signalling in peripheral Tregs is understudied (76,106–110). In the current study, it was observed that NRP1 inhibition in TCR+B16-F10-CS-treated peripheral splenic T cells downregulated expression of phosphorylated STAT3, STAT5 and STAT1 as compared to only TCR+B16-F10-CS treated ones (**Figure 5A-D**). Earlier findings suggested that upregulation in phosphorylated STAT3 and STAT5 expression in Tregs is mediated through IL-10 and TGF-β signalling and is reported to augment FOXP3 expression and immunosuppressive potential of Tregs (111,112). STAT1 was reported to exert complex functions on both tumour cells and the immune system and is usually considered a tumour suppressor. However, inappropriate activation of STAT1 has been observed in various malignant cells, including those from breast cancer, head and neck squamous carcinoma, melanoma, lymphoma, and leukaemia. This suggested that STAT1 may, under specific conditions, contribute to rather than inhibit malignant transformation. Additionally, STAT1 was reported to play a vital role in inducing the expression of IDO that enhanced tryptophan catabolism-mediated T-cell activation blockade (107). Therefore, it might indicate that EG-mediated NRP1 inhibition in TCR+B16-F10-CS-treated peripheral splenic Tregs downregulated STAT, Smad2/3 and ERK pathways that are reported to aid in immunosuppression in Tregs. It also upregulated AKT/PI3K pathways that are reported to destabilise FOXP3 expressing Tregs (113).

NRP1 also inhibited the immunosuppressive Treg population in intratumoral regions in different cancers (69,71,79,81–84). The current study depicted its possible role in regulating the expression of immunosuppressive markers in peripheral splenic Tregs. Peripheral splenic T cells isolated from EG-

treated B16-F10 tumour-bearing mice showed alleviated not only expression of different IRs like NRP1, NKG2A, FOXP3, PD-1, PD-L1 and CTLA-4 but also Th_2 marker GATA-3 (**Figure 6A-G and Supplementary figure S9A-G**). Therefore, it was found that NRP1 inhibition downregulated the expression of IRs in peripheral Tregs as well. Moreover, although T-bet is known to be a marker for Tregs, it is reported to facilitate Th_1 responses in Tregs (114). Interestingly, peripheral splenic T cells isolated from EG-treated B16-F10 tumour-bearing mice showed elevated expression of T-bet (**Figure 6H and Supplementary figure S4H**). Therefore, it was observed that NRP1 inhibition aided in promoting Th_1 responses in Tregs that might help in anti-tumour activity since prolonged exposure to Th_1 conditions was reported to be essential for sustained tumour-specific cytotoxic T lymphocyte activity (115).

Additionally, it was observed that peripheral splenic T cells isolated from EG-treated B16-F10 tumour-bearing mice showed elevated T cell proliferation (**Figure 7A and Supplementary figure S10A)**. It was also found that while there was a significant increase in $CD4^+$ T cells in the spleens of tumour-bearing mice compared to control mice, there was no change in $CD4^+$ T cell count in the spleens of untreated and EG-treated tumour-bearing mice (**Supplementary figure S5A and C**). However, the total number of $CD4^+$ $NRP1^+$ Tregs was lower in the spleens of EG-treated tumour-bearing mice than those untreated (**Supplementary figure S6A and C**). These cells isolated from spleens of EG-treated tumour-bearing mice containing a lower number of $CD4^+$ $NRP1^+$ Tregs also enhanced the proliferation of TCR-activated CFSE-labelled effector T cells (**Figure 7B and Supplementary figure S7B**). Thus, EG treatment in B16-F10 tumour-bearing mice increased peripheral splenic T cell proliferation and reduced Treg suppressive activity, unlike splenic T cells from untreated B16-F10 tumour-bearing mice. Overall, EG treatment augmented effector T cell proliferation and mitigated Treg suppressive activity in both *in vitro* and *in vivo* peripheral Tregs.

NRP1 has been reported as a potential target for melanoma (44,69,116). Repurposed drugs like gliclazide and entrectenib have shown significant anti-tumour activity in metastatic melanoma by preventing the PDGF-C/NRP1 interaction (43). However, the possible anti-tumour activity of EG on melanoma has not been deciphered yet. It was observed that EG treatment diminished B16-F10 lung metastasis in syngenic C57BL/6 mice and reduced the formation of metastatic lung nodules (Figures **8A and D**). EG treatment also regressed the B16-F10-melanoma tumour volume (**Figure 8B and F and Supplementary figure S11**). Additionally, EG treatment enhanced the survivability of C57BL/6 mice injected with B16-F10 melanoma cells either intravenously or subcutaneously (**Figure 8C and E**). This might be due to tumour cell death, as depicted in our findings, ameliorated peripheral Treg-mediated immunosuppression or both (**Figure 2D, 4, 6 and 7**).

The current study demonstrated for the first time that EG treatment might regulate peripheral Treg-mediated immunosuppression and inhibit B16-F10 melanoma tumour growth and metastasis while improving survival. Nonetheless, the possible regulation of EG-mediated NRP1 inhibition in intratumoral Tregs and possible anti-tumoral activity of EG against melanoma cancer in mice as well as in humans is to be conducted for a better evaluation of EG as a potential anti-cancer immunotherapeutic strategy. Moreover, as reported earlier (42), EG might be formulated with better delivery molecules to improve their dosage and efficient drug concentration. Furthermore, EG, in combination with other ICIs, must be examined for possible enhanced efficacy without causing any deleterious side effects, as seen for other ICIs.

Conclusion

This study showed for the first time that EG treatment may control peripheral Treg-mediated immune suppression, slow the growth and spread of B16-F10 melanoma tumours, and help improve survival. This might highlight the potential of NRP1 as a promising anti-cancerous immunotherapeutic target, alone or in combination with the current standard therapeutic regimen.

Funding

The work has been supported by the Department of Atomic Energy (DAE), a fellowship from DST INSPIRE to Somlata Khamaru, Govt. of India.

Ethics statement

The animal study was reviewed and approved by the Institutional Animal Ethics Committee, NISER (1634/GO/ReBi/S/12/CPSCEA) under the affiliation of the Committee for the Control and Supervision of Experiments on Animals (CCSEA) of India.

Authors contribution

Somlata Khamaru: Contributed majorly to conceptualisation, design, all experimentation, data acquisition, data analysis, manuscript writing and editing. **Kshyama Subhadarsini Tung**: Contributed to manuscript writing, reviewing and editing. **Subhasis Chattopadhyay**: Contributed to conceiving, conceptualising, design of the study, fund acquisition, manuscript review and editing.

Acknowledgement

The authors are thankful towards NISER Flowcytometry and the Animal House facility for providing pivotal support to conduct the study.

Declaration of competing interest

The authors declare that they have no known competing financial interests or personal relationships that could have appeared to influence the work reported in this paper.

Data availability

The original contributions presented in the study are included in the article/Supplementary Material. Further inquiries can be directed to the corresponding authors.

References

1. Matthews NH, Li W-Q, Qureshi AA, Weinstock MA, Cho E. Epidemiology of Melanoma. Prog Clin Cancer [Internet]. Codon Publications; 2017 [cited 2024 Jul 7];6:139–49. Available from: https://www.ncbi.nlm.nih.gov/books/NBK481862/

2. Kubica AW, Brewer JD. Melanoma in Immunosuppressed Patients. Mayo Clin Proc [Internet]. Mayo Foundation; 2012 [cited 2024 Jul 27];87:991. Available from: /pmc/articles/PMC3538393/

3. Chattopadhyay S, Chakraborty NG, Mukherji B. Regulatory T cells and tumor immunity. Cancer Immunology, Immunotherapy [Internet]. Springer; 2005 [cited 2024 Aug 26];54:1153–61. Available from: https://link.springer.com/article/10.1007/s00262-005-0699-9

4. Chattopadhyay S, Mehrotra S, Chhabra A, Hegde U, Mukherji B, Chakraborty NG. Effect of CD4+CD25+ and CD4+CD25− T Regulatory Cells on the Generation of Cytolytic T Cell Response to a Self but Human Tumor-Associated Epitope In Vitro. The Journal of Immunology [Internet]. American Association of Immunologists; 2006 [cited 2024 Aug 26];176:984–90. Available from: https://dx.doi.org/10.4049/jimmunol.176.2.984

5. Dong H, Strome SE, Salomao DR, Tamura H, Hirano F, Flies DB, et al. Tumor-associated B7-H1 promotes T-cell apoptosis: A potential mechanism of immune evasion. Nature Medicine 2002 8:8 [Internet]. Nature Publishing Group; 2002 [cited 2024 Jul 28];8:793–800. Available from: https://www.nature.com/articles/nm730

6. Piao W, Li L, Saxena V, Iyyathurai J, Lakhan R, Zhang Y, et al. PD-L1 signaling selectively regulates T cell lymphatic transendothelial migration. Nat Commun [Internet]. Nature Publishing Group; 2022 [cited 2024 Jul 28];13. Available from: /pmc/articles/PMC9023578/

7. Roy S, Bag AK, Singh RK, Talmadge JE, Batra SK, Datta K. Multifaceted Role of Neuropilins in the Immune System: Potential Targets for Immunotherapy. Front Immunol [Internet]. Frontiers Media SA; 2017 [cited 2024 Jul 25];8:1228. Available from: /pmc/articles/PMC5641316/

8. Cinier J, Hubert M, Besson L, Roio A Di, Rodriguez C, Lombardi V, et al. cancers Recruitment and Expansion of Tregs Cells in the Tumor Environment-How to Target Them? Cancers (Basel). 2021;13:1850.

9. Facciabene A, Motz GT, Coukos G. T-regulatory cells: key players in tumor immune escape and angiogenesis. Cancer Res. 2012;72:2162–71.

10. Curiel TJ, Coukos G, Zou L, Alvarez X, Cheng P, Mottram P, et al. Specific recruitment of regulatory T cells in ovarian carcinoma fosters immune privilege and predicts reduced survival. Nat Med. 2004;10:942–9.

849 11. Yamaguchi H, Hsu J-M, Sun L, Wang S-C, Hung M-C. Advances and prospects of biomarkers for
850 immune checkpoint inhibitors. Cell Rep Med [Internet]. Elsevier; 2024 [cited 2024 Jul 8];0:101621.
851 Available from: http://www.cell.com/article/S2666379124003252/fulltext

852 12. Carlino MS, Larkin J, Long G V. Immune checkpoint inhibitors in melanoma. Lancet [Internet]. Lancet;
853 2021 [cited 2024 Jul 8];398:1002–14. Available from: https://pubmed.ncbi.nlm.nih.gov/34509219/

854 13. Vinay DS, Ryan EP, Pawelec G, Talib WH, Stagg J, Elkord E, et al. Immune evasion in cancer:
855 Mechanistic basis and therapeutic strategies. Semin Cancer Biol. Academic Press; 2015;35:S185–98.

856 14. Mattia G, Puglisi R, Ascione B, Malorni W, Carè A, Matarrese P. Cell death-based treatments of
857 melanoma:conventional treatments and new therapeutic strategies. Cell Death & Disease 2018 9:2
858 [Internet]. Nature Publishing Group; 2018 [cited 2024 Jul 7];9:1–14. Available from:
859 https://www.nature.com/articles/s41419-017-0059-7

860 15. Waldman AD, Fritz JM, Lenardo MJ. A guide to cancer immunotherapy: from T cell basic science to
861 clinical practice. Nature Reviews Immunology 2020 20:11 [Internet]. Nature Publishing Group; 2020
862 [cited 2024 Jul 7];20:651–68. Available from: https://www.nature.com/articles/s41577-020-0306-5

863 16. Paluskievicz CM, Cao X, Abdi R, Zheng P, Liu Y, Bromberg JS. T regulatory cells and priming the
864 suppressive tumor microenvironment. Front Immunol [Internet]. Frontiers Media S.A.; 2019 [cited
865 2024 Jul 7];10:488694. Available from: www.frontiersin.org

866 17. Das M, Zhu C, Kuchroo VK. Tim-3 and its role in regulating anti-tumor immunity. Immunol Rev
867 [Internet]. NIH Public Access; 2017 [cited 2024 Jul 27];276:97. Available from:
868 /pmc/articles/PMC5512889/

869 18. Mulati K, Hamanishi J, Matsumura N, Chamoto K, Mise N, Abiko K, et al. VISTA expressed in tumour
870 cells regulates T cell function. British Journal of Cancer 2018 120:1 [Internet]. Nature Publishing
871 Group; 2018 [cited 2024 Jul 27];120:115–27. Available from:
872 https://www.nature.com/articles/s41416-018-0313-5

873 19. Liu Z, Zhou J, Wu S, Chen Z, Wu S, Chen L, et al. Why Treg should be the focus of cancer
874 immunotherapy: The latest thought. Biomedicine & Pharmacotherapy. Elsevier Masson;
875 2023;168:115142.

876 20. Suman S, Markovic SN. Melanoma-derived mediators can foster the premetastatic niche: crossroad to
877 lymphatic metastasis. Trends Immunol [Internet]. Elsevier Ltd; 2023 [cited 2024 Jul 28];44:724–43.
878 Available from: http://www.cell.com/article/S1471490623001369/fulltext

879 21. Huang AC, Zappasodi R. A decade of checkpoint blockade immunotherapy in melanoma:
880 understanding the molecular basis for immune sensitivity and resistance. Nature Immunology 2022
881 23:5 [Internet]. Nature Publishing Group; 2022 [cited 2024 Jul 8];23:660–70. Available from:
882 https://www.nature.com/articles/s41590-022-01141-1

883 22. Dobosz P, Stępień M, Golke A, Dzieciątkowski T. Challenges of the Immunotherapy: Perspectives and
884 Limitations of the Immune Checkpoint Inhibitor Treatment. Int J Mol Sci [Internet]. Multidisciplinary
885 Digital Publishing Institute (MDPI); 2022 [cited 2024 Jul 8];23:23. Available from:
886 /pmc/articles/PMC8910928/

887 23. Chuckran CA, Liu C, Bruno TC, Workman CJ, Vignali DAA. Neuropilin-1: A checkpoint target with
888 unique implications for cancer immunology and immunotherapy. J Immunother Cancer. BMJ
889 Publishing Group; 2020;8.

890 24. Nakamura F, Goshima Y. Structural and Functional Relation of Neuropilins. Landes Bioscience; 2013
891 [cited 2024 Jul 7]; Available from: https://www.ncbi.nlm.nih.gov/books/NBK6408/

892 25. Douyère M, Chastagner P, Boura C. Neuropilin-1: A Key Protein to Consider in the Progression of
893 Pediatric Brain Tumors. Front Oncol [Internet]. Frontiers Media S.A.; 2021 [cited 2024 Jul
894 8];11:665634. Available from: www.frontiersin.org

895 26. Delgoffe GM, Woo SR, Turnis ME, Gravano DM, Guy C, Overacre AE, et al. Stability and function of
896 regulatory T cells is maintained by a neuropilin-1–semaphorin-4a axis. Nature 2013 501:7466
897 [Internet]. Nature Publishing Group; 2013 [cited 2024 Jul 28];501:252–6. Available from:
898 https://www.nature.com/articles/nature12428

899 27. Mccarty O, Postow M, Lacal PM, Graziani G. MINI REVIEW Neuropilin-1 as therapeutic target for
900 malignant melanoma. 2015 [cited 2024 Jul 8]; Available from: www.frontiersin.org

901 28. Liu SD, Zhong LP, He J, Zhao YX. Targeting neuropilin-1 interactions is a promising anti-tumor strategy.
902 Chin Med J (Engl) [Internet]. Wolters Kluwer Health; 2021 [cited 2024 Jul 31];134:508. Available from:
903 /pmc/articles/PMC7929525/

904 29. Zhang P, Chen L, Zhou F, He Z, Wang G, Luo Y. NRP1 promotes prostate cancer progression via
905 modulating EGFR-dependent AKT pathway activation. Cell Death & Disease 2023 14:2 [Internet].
906 Nature Publishing Group; 2023 [cited 2024 Jul 25];14:1–16. Available from:
907 https://www.nature.com/articles/s41419-023-05696-1

908 30. Li L, Jiang X, Zhang Q, Dong X, Gao Y, He Y, et al. Neuropilin-1 is associated with clinicopathology of
909 gastric cancer and contributes to cell proliferation and migration as multifunctional co-receptors.
910 Journal of Experimental and Clinical Cancer Research. BioMed Central Ltd.; 2016;35.

911 31. Dumond A, Pagès G. Neuropilins, as Relevant Oncology Target: Their Role in the Tumoral
912 Microenvironment. Front Cell Dev Biol [Internet]. Frontiers Media S.A.; 2020 [cited 2024 Jul
913 25];8:561700. Available from: www.frontiersin.org

914 32. De Vlaeminck Y, Bonelli S, Awad RM, Dewilde M, Rizzolio S, Lecocq Q, et al. Targeting Neuropilin-1
915 with Nanobodies Reduces Colorectal Carcinoma Development. Cancers 2020, Vol 12, Page 3582
916 [Internet]. Multidisciplinary Digital Publishing Institute; 2020 [cited 2024 Jul 25];12:3582. Available
917 from: https://www.mdpi.com/2072-6694/12/12/3582/htm

918 33. Rodrigues EM, Giovanini AF, Ribas CAPM, Malafaia O, Roesler R, Isolan GR. The Nervous System
919 Development Regulator Neuropilin-1 as a Potential Prognostic Marker and Therapeutic Target in Brain
920 Cancer. Cancers (Basel) [Internet]. Multidisciplinary Digital Publishing Institute (MDPI); 2023 [cited
921 2024 Jul 25];15. Available from: /pmc/articles/PMC10605093/

922 34. Hong TM, Chen YL, Wu YY, Yuan A, Chao YC, Chung YC, et al. Targeting Neuropilin 1 as an Antitumor
923 Strategy in Lung Cancer. Clinical Cancer Research [Internet]. American Association for Cancer
924 Research; 2007 [cited 2024 Jul 23];13:4759–68. Available from:
925 /clincancerres/article/13/16/4759/12947/Targeting-Neuropilin-1-as-an-Antitumor-Strategy-in

926 35. Wu Q, Pan C, Zhou Y, Wang S, Xie L, Zhou W, et al. Targeting neuropilin-1 abolishes anti-PD-1-
927 upregulated regulatory T cells and synergizes with 4-1BB agonist for liver cancer treatment.
928 Hepatology [Internet]. Hepatology; 2023 [cited 2024 Jul 23];78:1402–17. Available from:
929 https://pubmed.ncbi.nlm.nih.gov/36811396/

930 36. Zhang P, Chen L, Zhou F, He Z, Wang G, Luo Y. NRP1 promotes prostate cancer progression via
931 modulating EGFR-dependent AKT pathway activation. Cell Death & Disease 2023 14:2 [Internet].

932 Nature Publishing Group; 2023 [cited 2024 Jul 23];14:1–16. Available from:
933 https://www.nature.com/articles/s41419-023-05696-1

934 37. Jung K, Kim JA, Kim YJ, Lee HW, Kim CH, Haam S, et al. A neuropilin-1 antagonist exerts antitumor
935 immunity by inhibiting the suppressive function of intratumoral regulatory T cells. Cancer Immunol
936 Res [Internet]. American Association for Cancer Research Inc.; 2020 [cited 2024 Jul 23];8:46–56.
937 Available from: /cancerimmunolres/article/8/1/46/469552/A-Neuropilin-1-Antagonist-Exerts-
938 Antitumor

939 38. Huang Z, Cheng C, Xiong H, Wang Y, Chen KK, Yang J, et al. NRP1 promotes cell migration and invasion
940 and serves as a therapeutic target in nasopharyngeal carcinoma. Int J Clin Exp Pathol [Internet]. e-
941 Century Publishing Corporation; 2018 [cited 2024 Jul 27];11:2460. Available from:
942 /pmc/articles/PMC6958308/

943 39. Powell J, Mota F, Steadman D, Soudy C, Miyauchi JT, Crosby S, et al. Small Molecule Neuropilin-1
944 Antagonists Combine Antiangiogenic and Antitumor Activity with Immune Modulation through
945 Reduction of Transforming Growth Factor Beta (TGFβ) Production in Regulatory T-Cells. J Med Chem
946 [Internet]. J Med Chem; 2018 [cited 2024 Jul 27];61:4135–54. Available from:
947 https://pubmed.ncbi.nlm.nih.gov/29648813/

948 40. Cong L, Yi J, Qiu S, Wang R, Jin S, Jiang R, et al. Effect of EG00229 on Radiation Resistance of Lung
949 Adenocarcinoma Cells. J Cancer [Internet]. Ivyspring International Publisher; 2021 [cited 2024 Jul
950 27];12:6105. Available from: /pmc/articles/PMC8425201/

951 41. Zheng C, Wang H, Zhao S, Ma C, Gao H, Yang F, et al. Inhibition of neuropilin-1 enhances the
952 therapeutic effects of lenvatinib in suppressing cholangiocarcinoma cells via the c-Met pathway. Eur J
953 Pharmacol. Elsevier; 2022;935:175290.

954 42. Pal K, Madamsetty VS, Dutta SK, Wang E, Angom RS, Mukhopadhyay D. Synchronous inhibition of
955 mTOR and VEGF/NRP1 axis impedes tumor growth and metastasis in renal cancer. npj Precision
956 Oncology 2019 3:1 [Internet]. Nature Publishing Group; 2019 [cited 2024 Jul 31];3:1–11. Available
957 from: https://www.nature.com/articles/s41698-019-0105-2

958 43. Ceci C, Ruffini F, Falconi M, Grazia Atzori M, Falzon A, Lozzi F, et al. Pharmacological inhibition of PDGF-
959 C/neuropilin-1 interaction: A novel strategy to reduce melanoma metastatic potential. Biomedicine &
960 Pharmacotherapy. Elsevier Masson; 2024;176:116766.

961 44. Graziani G, Lacal PM. Neuropilin-1 as therapeutic target for malignant melanoma. Front Oncol
962 [Internet]. Frontiers Media S.A.; 2015 [cited 2024 Jul 16];5:149115. Available from:
963 www.frontiersin.org

964 45. Rodrigues EM, Giovanini AF, Ribas CAPM, Malafaia O, Roesler R, Isolan GR. The Nervous System
965 Development Regulator Neuropilin-1 as a Potential Prognostic Marker and Therapeutic Target in Brain
966 Cancer. Cancers (Basel) [Internet]. Multidisciplinary Digital Publishing Institute (MDPI); 2023 [cited
967 2024 Jul 23];15. Available from: /pmc/articles/PMC10605093/

968 46. Cong L, Yi J, Qiu S, Wang R, Jin S, Jiang R, et al. Effect of EG00229 on Radiation Resistance of Lung
969 Adenocarcinoma Cells. J Cancer [Internet]. Ivyspring International Publisher; 2021 [cited 2024 Jul
970 28];12:6105. Available from: /pmc/articles/PMC8425201/

971 47. Benwell CJ, Johnson RT, Taylor JAGE, Price CA, Robinson SD. Endothelial VEGFR Coreceptors
972 Neuropilin-1 and Neuropilin-2 Are Essential for Tumor Angiogenesis. Cancer Research
973 Communications [Internet]. American Association for Cancer Research Inc.; 2022 [cited 2024 Jul

31];2:1626–40. Available from: /cancerrescommun/article/2/12/1626/711639/Endothelial-VEGFR-Coreceptors-Neuropilin-1-and

48. B16-F10 - CRL-6475 | ATCC [Internet]. [cited 2024 Apr 24]. Available from: https://www.atcc.org/products/crl-6475

49. NIH/3T3 - CRL-1658 | ATCC [Internet]. [cited 2024 Apr 24]. Available from: https://www.atcc.org/products/crl-1658

50. Kumar PS, Mukherjee T, Khamaru S, Radhakrishnan A, Kishore DJN, Chawla S, et al. Elevation of TRPV1 expression on T-cells during experimental immunosuppression. J Biosci [Internet]. Springer; 2022 [cited 2022 Dec 25];47:1–12. Available from: https://link.springer.com/article/10.1007/s12038-022-00279-2

51. Gao R, Ma J, Wen Z, Yang P, Zhao J, Xue M, et al. Tumor cell-released autophagosomes (TRAP) enhance apoptosis and immunosuppressive functions of neutrophils. Oncoimmunology [Internet]. Taylor and Francis Inc.; 2018 [cited 2022 Dec 24];7. Available from: https://www.tandfonline.com/doi/abs/10.1080/2162402X.2018.1438108

52. Overwijk WW, Restifo NP. B16 as a Mouse Model for Human Melanoma. Curr Protoc Immunol [Internet]. John Wiley & Sons, Ltd; 2000 [cited 2024 Aug 3];39:20.1.1-20.1.29. Available from: https://onlinelibrary.wiley.com/doi/full/10.1002/0471142735.im2001s39

53. Zhang J, Qiu J, Zhou W, Cao J, Hu X, Mi W, et al. Neuropilin-1 mediates lung tissue-specific control of ILC2 function in type 2 immunity. Nature Immunology 2022 23:2 [Internet]. Nature Publishing Group; 2022 [cited 2024 Aug 26];23:237–50. Available from: https://www.nature.com/articles/s41590-021-01097-8

54. Grun D, Adhikary G, Eckert RL. VEGF-A acts via neuropilin-1 to enhance epidermal cancer stem cell survival and formation of aggressive and highly vascularized tumors. Oncogene [Internet]. NIH Public Access; 2016 [cited 2024 Aug 26];35:4379. Available from: /pmc/articles/PMC4959993/

55. Sahoo SS, Pratheek BM, Meena VS, Nayak TK, Kumar PS, Bandyopadhyay S, et al. VIPER regulates naive T cell activation and effector responses: Implication in TLR4 associated acute stage T cell responses. Sci Rep [Internet]. 2018;8:7118. Available from: https://doi.org/10.1038/s41598-018-25549-8

56. Dragoni S, Brash JT, Fantin A, Burridge C, Denti L, Turowski P, et al. Targeting NRP1 with EG00229 induces neurovascular permeability. bioRxiv [Internet]. Cold Spring Harbor Laboratory; 2024 [cited 2024 Aug 26];2023.11.07.564946. Available from: https://www.biorxiv.org/content/10.1101/2023.11.07.564946v2

57. Nayak TK, Mamidi P, Kumar A, Singh LPK, Sahoo SS, Chattopadhyay S, et al. Regulation of Viral Replication, Apoptosis and Pro-Inflammatory Responses by 17-AAG during Chikungunya Virus Infection in Macrophages. Viruses 2017, Vol 9, Page 3 [Internet]. Multidisciplinary Digital Publishing Institute; 2017 [cited 2022 Dec 22];9:3. Available from: https://www.mdpi.com/1999-4915/9/1/3/htm

58. Majhi RK, Sahoo SS, Yadav M, Pratheek BM, Chattopadhyay S, Goswami C. Functional expression of TRPV channels in T cells and their implications in immune regulation. FEBS J [Internet]. John Wiley & Sons, Ltd; 2015 [cited 2022 Dec 23];282:2661–81. Available from: https://onlinelibrary.wiley.com/doi/full/10.1111/febs.13306

59. BD Cytometric Bead Array (CBA) Mouse Th1/Th2/Th17 Cytokine Kit Instruction Manual. 2009.

1015 60. Baumgartner J, Wilson C, Palmer B, Richter D, Banerjee A, McCarter M. Melanoma Induces
1016 Immunosuppression by Up-Regulating FOXP3+ Regulatory T Cells. Journal of Surgical Research.
1017 Academic Press; 2007;141:72–7.

1018 61. Rodriguez-Garcia GJ, Graves DK, Mirza MB, Idrees K, Kim YJ, Korrer MJ, et al. Cancer Cell Small
1019 Molecule Secretome Induces the Immune Checkpoint NKG2A and Dysfunction of Human CD8+ T Cells.
1020 Immunohorizons [Internet]. American Association of Immunologists; 2024 [cited 2024 Jul 10];8:464–
1021 77. Available from: https://dx.doi.org/10.4049/immunohorizons.2400046

1022 62. Yuan XL, Chen L, Zhang TT, Ma YH, Zhou YL, Zhao Y, et al. Gastric cancer cells induce human
1023 CD4+Foxp3+ regulatory T cells through the production of TGF-β1. World Journal of Gastroenterology:
1024 WJG [Internet]. Baishideng Publishing Group Inc; 2011 [cited 2024 Jul 10];17:2019. Available from:
1025 /pmc/articles/PMC3082757/

1026 63. Sun LX, Lin Z Bin, Duan XS, Lu J, Ge ZH, Li XJ, et al. Ganoderma lucidum polysaccharides antagonize the
1027 suppression on lymphocytes induced by culture supernatants of B16F10 melanoma cells. Journal of
1028 Pharmacy and Pharmacology [Internet]. Oxford Academic; 2011 [cited 2022 Dec 9];63:725–35.
1029 Available from: https://academic.oup.com/jpp/article/63/5/725/6135570

1030 64. Ruffini F, D'Atri S, Lacal PM. Neuropilin-1 expression promotes invasiveness of melanoma cells through
1031 vascular endothelial growth factor receptor-2-dependent and -independent mechanisms. Int J Oncol
1032 [Internet]. Spandidos Publications; 2013 [cited 2024 Jul 16];43:297–306. Available from:
1033 http://www.spandidos-publications.com/10.3892/ijo.2013.1948/abstract

1034 65. Rizzolio S, Cagnoni G, Battistini C, Bonelli S, Isella C, Van Ginderachter JA, et al. Neuropilin-1
1035 upregulation elicits adaptive resistance to oncogene-targeted therapies. J Clin Invest [Internet].
1036 American Society for Clinical Investigation; 2018 [cited 2024 Jul 27];128:3976–90. Available from:
1037 https://doi.org/10.1172/JCI99257.

1038 66. Sidaway P. Neuropilin-1 is required for Treg stability. Nature Reviews Clinical Oncology 2017 14:8
1039 [Internet]. Nature Publishing Group; 2017 [cited 2024 Jul 18];14:458–458. Available from:
1040 https://www.nature.com/articles/nrclinonc.2017.90

1041 67. Overacre-Delgoffe AE, Chikina M, Dadey RE, Yano H, Brunazzi EA, Shayan G, et al. Interferon-γ Drives
1042 Treg Fragility to Promote Anti-tumor Immunity. Cell [Internet]. Cell; 2017 [cited 2024 Jul 18];169:1130-
1043 1141.e11. Available from: https://pubmed.ncbi.nlm.nih.gov/28552348/

1044 68. Overacre AE, Vignali DAA. TREG STABILITY: TO BE OR NOT TO BE. Curr Opin Immunol [Internet]. NIH
1045 Public Access; 2016 [cited 2024 Jul 18];39:39. Available from: /pmc/articles/PMC4801724/

1046 69. Hansen W, Hutzler M, Abel S, Alter C, Stockmann C, Kliche S, et al. Neuropilin 1 deficiency on
1047 CD4+Foxp3+ regulatory T cells impairs mouse melanoma growth. J Exp Med [Internet]. The
1048 Rockefeller University Press; 2012 [cited 2024 Jul 18];209:2001. Available from:
1049 /pmc/articles/PMC3478934/

1050 70. Milpied P, Massot B, Renand A, Diem S, Herbelin A, Leite-de-Moraes M, et al. IL-17–producing
1051 invariant NKT cells in lymphoid organs are recent thymic emigrants identified by neuropilin-1
1052 expression. Blood [Internet]. American Society of Hematology; 2011 [cited 2024 Jul 18];118:2993–
1053 3002. Available from: https://dx.doi.org/10.1182/blood-2011-01-329268

1054 71. Borst L, Sluijter M, Sturm G, Charoentong P, Santegoets SJ, van Gulijk M, et al. NKG2A is a late immune
1055 checkpoint on CD8 T cells and marks repeated stimulation and cell division. Int J Cancer [Internet].
1056 John Wiley & Sons, Ltd; 2022 [cited 2024 Jul 24];150:688–704. Available from:
1057 https://onlinelibrary.wiley.com/doi/full/10.1002/ijc.33859

1058 72. Chen W, Huang W, Xue Y, Chen Y, Qian W, Ma J, et al. Neuropilin-1 Identifies a New Subpopulation of
1059 TGF-β-Induced Foxp3+ Regulatory T Cells With Potent Suppressive Function and Enhanced Stability
1060 During Inflammation. Front Immunol [Internet]. Frontiers Media S.A.; 2022 [cited 2024 Jul
1061 24];13:900139. Available from: www.frontiersin.org

1062 73. Liu SD, Zhong LP, He J, Zhao YX. Targeting neuropilin-1 interactions is a promising anti-tumor strategy.
1063 Chin Med J (Engl) [Internet]. Wolters Kluwer Health; 2021 [cited 2024 Jul 19];134:508. Available from:
1064 /pmc/articles/PMC7929525/

1065 74. Overacre-Delgoffe AE, Chikina M, Dadey RE, Yano H, Brunazzi EA, Shayan G, et al. Interferon-γ Drives
1066 Treg Fragility to Promote Anti-tumor Immunity. Cell [Internet]. Cell; 2017 [cited 2024 Jul 31];169:1130-
1067 1141.e11. Available from: https://pubmed.ncbi.nlm.nih.gov/28552348/

1068 75. Xiao S, Yang Y, Miao W, Lyu C, Tao J, Yu Y. Activation of the STAT5 Signaling Pathway by Yiqi Jiedu
1069 Formula Induces Regulatory T Cell-Mediated Alleviation of Corneal Immunopathological Damage in
1070 Mice With Recurrent Herpes Simplex Keratitis. Front Pharmacol. Frontiers Media S.A.; 2022;12.

1071 76. Huang P, Zhang L, Wang H, Dou C, Ju H, Yue P, et al. Neuropilin-1 enhances temozolomide resistance in
1072 glioblastoma via the STAT1/p53/p21 axis. Neuropathology [Internet]. John Wiley & Sons, Ltd; 2024
1073 [cited 2024 Jul 23]; Available from: https://onlinelibrary.wiley.com/doi/full/10.1111/neup.12966

1074 77. Yang Y, Yang L, Li Y. Neuropilin-1 (NRP-1) upregulated by IL-6/STAT3 signaling contributes to invasion in
1075 pancreatic neuroendocrine neoplasms. Hum Pathol. W.B. Saunders; 2018;81:192–200.

1076 78. Meng S, Hara T, Sato H, Tatekawa S, Tsuji Y, Saito Y, et al. Revealing neuropilin expression patterns in
1077 pancreatic cancer: From single-cell to therapeutic opportunities (Review). Oncol Lett [Internet].
1078 Spandidos Publications; 2024 [cited 2024 Jul 23];27:1–81. Available from: http://www.spandidos-
1079 publications.com/10.3892/ol.2024.14247/abstract

1080 79. Dong Y, Ma WM, Shi ZD, Zhang ZG, Zhou JH, Li Y, et al. Role of NRP1 in Bladder Cancer Pathogenesis
1081 and Progression. Front Oncol [Internet]. Frontiers Media S.A.; 2021 [cited 2024 Jul 23];11:1. Available
1082 from: /pmc/articles/PMC8261128/

1083 80. Rizzolio S, Rabinowicz N, Rainero E, Lanzetti L, Serini G, Norman J, et al. Neuropilin-1-dependent
1084 regulation of EGF-receptor Signaling. Cancer Res [Internet]. American Association for Cancer
1085 Research; 2012 [cited 2024 Jul 23];72:5801–11. Available from:
1086 /cancerres/article/72/22/5801/577534/Neuropilin-1-Dependent-Regulation-of-EGF-Receptor

1087 81. Sjaastad LE, Owen DL, Tracy SI, Farrar MA. Phenotypic and Functional Diversity in Regulatory T Cells.
1088 Front Cell Dev Biol [Internet]. Frontiers Media SA; 2021 [cited 2024 Jul 24];9. Available from:
1089 /pmc/articles/PMC8495164/

1090 82. Pichler R, Gruenbacher G, Culig Z, Brunner A, Fuchs D, Fritz J, et al. Intratumoral Th2 predisposition
1091 combines with an increased Th1 functional phenotype in clinical response to intravesical BCG in
1092 bladder cancer. Cancer Immunology, Immunotherapy. Springer Science and Business Media
1093 Deutschland GmbH; 2017;66:427–40.

1094 83. Dyck L, Mills KHG. Immune checkpoints and their inhibition in cancer and infectious diseases. Eur J
1095 Immunol. Wiley-VCH Verlag; 2017;47:765–79.

1096 84. Saleh R, Toor SM, Khalaf S, Elkord E. Breast Cancer Cells and PD-1/PD-L1 Blockade Upregulate the
1097 Expression of PD-1, CTLA-4, TIM-3 and LAG-3 Immune Checkpoints in CD4+ T Cells. Vaccines 2019, Vol
1098 7, Page 149 [Internet]. Multidisciplinary Digital Publishing Institute; 2019 [cited 2024 Jul 24];7:149.
1099 Available from: https://www.mdpi.com/2076-393X/7/4/149/htm

1100 85. Wegrzyn AS, Kedzierska AE, Obojski A. Identification and classification of distinct surface markers of T
1101 regulatory cells. Front Immunol. Frontiers Media S.A.; 2023;13:1055805.

1102 86. Campos-Mora M, Contreras-Kallens P, Gálvez-Jirón F, Rojas M, Rojas C, Refisch A, et al. CD4+Foxp3+T
1103 regulatory cells promote transplantation tolerance by modulating effector CD4+ T cells in a neuropilin-
1104 1-dependent manner. Front Immunol. Frontiers Media S.A.; 2019;10.

1105 87. Pal K, Madamsetty VS, Dutta SK, Wang E, Angom RS, Mukhopadhyay D. Synchronous inhibition of
1106 mTOR and VEGF/NRP1 axis impedes tumor growth and metastasis in renal cancer. npj Precision
1107 Oncology 2019 3:1 [Internet]. Nature Publishing Group; 2019 [cited 2024 Jul 27];3:1–11. Available
1108 from: https://www.nature.com/articles/s41698-019-0105-2

1109 88. Zheng C, Wang H, Zhao S, Ma C, Gao H, Yang F, et al. Inhibition of neuropilin-1 enhances the
1110 therapeutic effects of lenvatinib in suppressing cholangiocarcinoma cells via the c-Met pathway. Eur J
1111 Pharmacol. Elsevier; 2022;935:175290.

1112 89. Cong L, Yi J, Qiu S, Wang R, Jin S, Jiang R, et al. Effect of EG00229 on Radiation Resistance of Lung
1113 Adenocarcinoma Cells. J Cancer [Internet]. Ivyspring International Publisher; 2021 [cited 2024 Jul
1114 31];12:6105. Available from: /pmc/articles/PMC8425201/

1115 90. Sung H, Ferlay J, Siegel RL, Laversanne M, Soerjomataram I, Jemal A, et al. Global Cancer Statistics
1116 2020: GLOBOCAN Estimates of Incidence and Mortality Worldwide for 36 Cancers in 185 Countries. CA
1117 Cancer J Clin [Internet]. CA Cancer J Clin; 2021 [cited 2024 Jul 31];71:209–49. Available from:
1118 https://pubmed.ncbi.nlm.nih.gov/33538338/

1119 91. Delgoffe GM, Woo SR, Turnis ME, Gravano DM, Guy C, Overacre AE, et al. Stability and function of
1120 regulatory T cells is maintained by a neuropilin-1-semaphorin-4a axis. Nature. 2013;501:252–6.

1121 92. Liu SD, Zhong LP, He J, Zhao YX. Targeting neuropilin-1 interactions is a promising anti-tumor strategy.
1122 Chin Med J (Engl) [Internet]. Wolters Kluwer Health; 2021 [cited 2024 Jul 27];134:508. Available from:
1123 /pmc/articles/PMC7929525/

1124 93. Barman S, Das G, Gupta V, Mondal P, Jana B, Bhunia D, et al. Dual-Arm Nanocapsule Targets
1125 Neuropilin-1 Receptor and Microtubule: A Potential Nanomedicine Platform. Mol Pharm [Internet].
1126 Mol Pharm; 2019 [cited 2023 Mar 15];16:2522–31. Available from:
1127 https://pubmed.ncbi.nlm.nih.gov/31009223/

1128 94. Jung K, Kim JA, Kim YJ, Lee HW, Kim CH, Haam S, et al. A neuropilin-1 antagonist exerts antitumor
1129 immunity by inhibiting the suppressive function of intratumoral regulatory T cells. Cancer Immunol
1130 Res [Internet]. American Association for Cancer Research Inc.; 2020 [cited 2024 Jul 19];8:46–56.
1131 Available from: /cancerimmunolres/article/8/1/46/469552/A-Neuropilin-1-Antagonist-Exerts-
1132 Antitumor

1133 95. Rudensky AY. Regulatory T Cells and Foxp3. Immunol Rev [Internet]. NIH Public Access; 2011 [cited
1134 2024 Jul 31];241:260. Available from: /pmc/articles/PMC3077798/

1135 96. Benwell CJ, Johnson RT, Taylor JAGE, Price CA, Robinson SD. Endothelial VEGFR Coreceptors
1136 Neuropilin-1 and Neuropilin-2 Are Essential for Tumor Angiogenesis. Cancer Research
1137 Communications [Internet]. American Association for Cancer Research Inc.; 2022 [cited 2024 Jul
1138 28];2:1626–40. Available from: /cancerrescommun/article/2/12/1626/711639/Endothelial-VEGFR-
1139 Coreceptors-Neuropilin-1-and

1140 97. Cui H, Wang N, Li H, Bian Y, Wen W, Kong X, et al. The dynamic shifts of IL-10-producing Th17 and IL-
1141 17-producing Treg in health and disease: a crosstalk between ancient. Cell Communication and

1142 Signaling 2024 22:1 [Internet]. BioMed Central; 2024 [cited 2024 Aug 1];22:1–23. Available from:
1143 https://biosignaling.biomedcentral.com/articles/10.1186/s12964-024-01505-0

1144 98. Downs-Canner S, Berkey S, Delgoffe GM, Edwards RP, Curiel T, Odunsi K, et al. Suppressive IL-
1145 17A+Foxp3+ and ex-Th17 IL-17AnegFoxp3+ Treg cells are a source of tumour-associated Treg cells.
1146 Nature Communications 2017 8:1 [Internet]. Nature Publishing Group; 2017 [cited 2024 Jul 31];8:1–
1147 15. Available from: https://www.nature.com/articles/ncomms14649

1148 99. Jung MK, Kwak JE, Shin EC. IL-17A-Producing Foxp3+ Regulatory T Cells and Human Diseases. Immune
1149 Netw [Internet]. The Korean Association of Immunologists; 2017 [cited 2024 Jul 31];17:276. Available
1150 from: /pmc/articles/PMC5662777/

1151 100. Sionov RV, Fridlender ZG, Granot Z. The Multifaceted Roles Neutrophils Play in the Tumor
1152 Microenvironment. Cancer Microenvironment [Internet]. Springer; 2015 [cited 2023 Sep 15];8:125.
1153 Available from: /pmc/articles/PMC4714999/

1154 101. Huang S, Liu D, Han L, Deng J, Wang Z, Jiang J, et al. Decoding the potential role of regulatory T cells in
1155 sepsis-induced immunosuppression. Eur J Immunol [Internet]. John Wiley & Sons, Ltd; 2024 [cited
1156 2024 Jul 31];54:2350730. Available from:
1157 https://onlinelibrary.wiley.com/doi/full/10.1002/eji.202350730

1158 102. Chaudhary B, Khaled YS, Ammori BJ, Elkord E. Neuropilin 1: function and therapeutic potential in
1159 cancer. Cancer Immunol Immunother. 2014;63:81–99.

1160 103. Park MJ, Moon SJ, Lee EJ, Kim EK, Baek JA, Kim SY, et al. Daurinol attenuates autoimmune arthritis via
1161 stabilization of NRP1–PTEN–FoxP3 signaling in regulatory T cells. Front Immunol [Internet]. Frontiers
1162 Media S.A.; 2019 [cited 2024 Jul 31];10:1526. Available from: /pmc/articles/PMC6651269/

1163 104. Akagi M, Kawaguchi M, Liu W, McCarty MF, Takeda A, Fan F, et al. Induction of neuropilin-I and
1164 vascular endothelial growth factor by epidermal growth factor in human gastric cancer cells. Br J
1165 Cancer. 2003;88:796–802.

1166 105. Yoshizaki T, Motomura W, Tanno S, Kumei S, Yoshizaki Y, Tanno S, et al. Thiazolidinediones enhance
1167 vascular endothelial growth factor expression and induce cell growth inhibition in non-small-cell lung
1168 cancer cells. Journal of Experimental and Clinical Cancer Research [Internet]. BioMed Central; 2010
1169 [cited 2024 Jul 31];29:1–9. Available from: https://link.springer.com/articles/10.1186/1756-9966-29-
1170 22

1171 106. Yu H, Pardoll D, Jove R. STATs in cancer inflammation and immunity: a leading role for STAT3. Nat Rev
1172 Cancer [Internet]. NIH Public Access; 2009 [cited 2023 Sep 15];9:798. Available from:
1173 /pmc/articles/PMC4856025/

1174 107. Pensa S, Regis G, Boselli D, Novelli F, Poli V. STAT1 and STAT3 in Tumorigenesis: Two Sides of the Same
1175 Coin? Landes Bioscience; 2013 [cited 2024 Jul 31]; Available from:
1176 https://www.ncbi.nlm.nih.gov/books/NBK6568/

1177 108. Das M, Stephen-Victor E, Bayry J. Regulatory T cells do not suppress rather activate human basophils
1178 by IL-3 and STAT5-dependent mechanisms. Oncoimmunology [Internet]. Taylor & Francis; 2020 [cited
1179 2023 Sep 15];9:1–3. Available from: /pmc/articles/PMC7458635/

1180 109. Jin J, Li Y, Zhao Q, Chen Y, Fu S, Wu JB. Coordinated regulation of immune contexture: crosstalk
1181 between STAT3 and immune cells during breast cancer progression. Cell Commun Signal [Internet].
1182 BMC; 2021 [cited 2023 Sep 15];19:50. Available from: /pmc/articles/PMC8101191/

110. Tang Q, Li J, Zhu H, Li P, Zou Z, Xiao Y. Hmgb1-IL-23-IL-17-IL-6-Stat3 Axis Promotes Tumor Growth in Murine Models of Melanoma. Mediators Inflamm [Internet]. Hindawi Limited; 2013 [cited 2023 Sep 15];2013:13. Available from: /pmc/articles/PMC3888736/

111. Schmetterer KG, Pickl WF. The IL–10/STAT3 axis: Contributions to immune tolerance by thymus and peripherally derived regulatory T-cells. Eur J Immunol [Internet]. John Wiley & Sons, Ltd; 2017 [cited 2024 Jul 31];47:1256–65. Available from: https://onlinelibrary.wiley.com/doi/full/10.1002/eji.201646710

112. Zong Y, Deng K, Chong WP. Regulation of Treg cells by cytokine signaling and co-stimulatory molecules. Front Immunol. Frontiers Media SA; 2024;15:1387975.

113. Lim EL, Okkenhaug K. Phosphoinositide 3-kinase δ is a regulatory T-cell target in cancer immunotherapy. Immunology [Internet]. John Wiley & Sons, Ltd; 2019 [cited 2024 Aug 1];157:210–8. Available from: https://onlinelibrary.wiley.com/doi/full/10.1111/imm.13082

114. Wan YY. Regulatory T cells: immune suppression and beyond. Cell Mol Immunol [Internet]. Nature Publishing Group; 2010 [cited 2024 Jul 31];7:204. Available from: /pmc/articles/PMC2868372/

115. Chattopadhyay S, Chakraborty NG. Continuous Presence of Th1 Conditions Is Necessary for Longer Lasting Tumor-Specific CTL Activity in Stimulation Cultures With PBL. Hum Immunol. Elsevier; 2005;66:884–91.

116. Rossignol J, Belaid Z, Fouquet G, Guillem F, Rignault R, Milpied P, et al. Neuropilin-1 cooperates with PD-1 in CD8+ T cells predicting outcomes in melanoma patients treated with anti-PD1. iScience [Internet]. Elsevier Inc.; 2022 [cited 2024 Jul 16];25:104353. Available from: http://www.cell.com/article/S2589004222006241/fulltext

Figure legends

Figure 1: Elevation of frequency of suppressor T cells during B16-F10 cell culture supernatant (B16-F10-CS) treatment, *in vitro*. (A) Flow cytometric dot plots showing alterations in the frequency of FOXP3, NKG2A and NRP1 positive purified splenic T cell population with or without anti-CD3/CD28 antibodies and B16-F10-CS treatment. Bar graph representation of alteration in frequency of (B) FOXP3, (C) NKG2A and (D) NRP1 positive purified splenic T cell population with or without anti-CD3/CD28 antibodies and B16-F10-CS treatment. Representative bar diagrams are of three independent experiments. ns, non-significant; * $p < 0.05$; ** $p < 0.01$; *** $p < 0.001$; **** $p < 0.0001$.

Figure 2: Neuropillin-1 (NRP1) expression is upregulated in melanoma patients and cell lines, and its inhibition induced apoptosis in tumorigenic B16-F10 cells. (A) Oncoprint depicting the frequency and types of alterations of the NRP1 gene in 212 melanoma cancer and 2683 pan-cancer patient samples from the cBioPortal database. (B) Bar graph representation of alteration frequency of NRP1 gene in 2683 cancer patient samples from cBioPortal database. (C) Fold change in mRNA

expression of NRP1 gene when compared between tumorigenic B16-F10 and non-tumorigenic NIH-3T3 cells. (D) Bar graphs representing apoptosis in tumorigenic B16-F10 and non-tumorigenic NIH-3T3 cells upon treatment with different concentrations of NRP1 inhibitor EG00229, which is determined by Annexin & 7-AAD dual staining. Representative bar diagrams are of three independent experiments. ns, non-significant; * $p < 0.05$; ** $p < 0.01$; *** $p < 0.001$; **** $p < 0.0001$.

Figure 3: Inhibition of Neuropillin-1 (NRP1) alleviated expression of suppressor T cell markers in splenic T cells treated with B16-F10 cell culture supernatant (B16-F10-CS), *in vitro*. (A) Flowcytometric histogram plots depicting alterations in the expression of NRP1, NKG2A and FOXP3 in anti-CD3/CD28 antibodies and B16-F10-CS treated purified splenic T cell with or without NRP1 inhibition. Bar graph representation of alteration in expression of (B) NRP1, (C) NKG2A and (D) FOXP3 in anti-CD3/CD28 antibodies and B16-F10-CS treated purified splenic T cell with or without NRP1 inhibition. Representative bar diagrams are of three independent experiments. ns, non-significant; * $p < 0.05$; ** $p < 0.01$; *** $p < 0.001$; **** $p < 0.0001$.

Figure 4: Inhibition of Neuropilin-1 (NRP1) enhanced proinflammatory cytokine secretion and T cell proliferation while decreasing Treg suppressive activity and the release of immunosuppressive cytokines in splenic T cells treated with B16-F10 cell culture supernatant (B16-F10-CS), *in vitro*. Bar graphs depicting the alteration in (A) TNF (B) IFN-γ, (C) IL-10, (D) IL-2, (E) IL-17(A), and (F) IL-6 secretion levels in anti-CD3/CD28 antibodies and B16-F10-CS treated purified splenic T cell with or without NRP1 inhibition. (G) Bar graph depicting proliferation of T cells via CFSE proliferation assay upon treatment with anti-CD3/CD28 antibodies and B16-F10-CS with or without NRP1 inhibition. (H) Bar graph depicting proliferation of effector T cells co-cultured with purified splenic T cells treated with anti-CD3/CD28 antibodies and B16-F10-CS with or without NRP1 inhibition. Representative bar diagrams are of three independent experiments. ns, non-significant; * $p < 0.05$; ** $p < 0.01$; *** $p < 0.001$; **** $p < 0.0001$.

Figure 5: Inhibition of Neuropilin-1 (NRP1) alleviated the STAT, SMAD2/3, and ERK MAPK pathways while enhancing the AKT/PI3K pathway in splenic T cells treated with B16-F10 cell culture supernatant (B16-F10-CS), *in vitro*. (A) Western blots showing expression of phosphorylated STAT3, STAT5, STAT1, SMAD2/3, PI3K, AKT, SAPK/JNK, P38 and ERK in anti-CD3/CD28 antibodies and B16-F10-CS treated purified splenic T cell with or without NRP1 inhibition. Representative bar graphs are of three independent experiments, showing relative expression levels of (B) p-STAT3, (C) p-STAT5, (D) p-STAT1, (E) p-SMAD2/3, (F) p-PI3K, (G) p-AKT and (H) p-ERK when compared with expression of total STAT3, STAT5, STAT1, SMAD2/3,

PI3K, AKT and ERK respectively. B-actin was used as a loading control for this experiment. ns, non-significant; * $p < 0.05$; ** $p < 0.01$; *** $p < 0.001$; **** $p < 0.0001$.

Figure 6: Expression of suppressor T cell markers alleviated in splenic T cells isolated from B16-F10 subcutaneous tumour-bearing mice treated with Neuropillin-1 (NRP1) inhibitor. Bar graphs depicting the alteration in expression of (A) NRP1, (B) NKG2A, (C) FOXP3, (D) T-bet, (E) GATA-3, (F) CTLA-4, (G) PD-1 and (H) PD-L1 in purified splenic T cells isolated from control healthy and B16-F10 subcutaneous tumour bearing C57BL/6 mice with or without NRP1 inhibitor treatment. Representative bar diagrams are of three independent experiments. ns, non-significant; * $p < 0.05$; ** $p < 0.01$; *** $p < 0.001$; **** $p < 0.0001$.

Figure 7: Increase in proliferation and reduction in suppressive activity of Tregs of purified splenic T cells isolated from B16-F10 subcutaneous tumour-bearing mice treated with Neuropilin-1 (NRP1) inhibitor. (A) Flowcytometric histogram plots depicting proliferation of purified splenic T cells isolated from B16-F10 subcutaneous tumour-bearing mice with or without treatment with Neuropillin-1 (NRP1) inhibitor. (B) Flowcytometric histogram plots depicting proliferation of effector T cells cultured with purified T cells isolated from B16-F10 subcutaneous tumour-bearing mice with or without NRP1 inhibitor treatment.

Figure 8: Neuropillin-1 (NRP1) inhibitor treatment alleviated B16-F10 lung metastasis and subcutaneous tumour volume in C57BL/6 mice and increased its survival. (A) Representative lung images of healthy control mice and lungs extracted from untreated and NRP1-treated C57BL/6 mice previously injected with B16-F10 cells intravenously. (B) Kaplan-Meier plot depicting the probability of survival of C57BL/6 mice with or without NRP1 inhibitor treatment after inoculation of $0.1X10^6$ B16-F10 cells intravenously. (C) Bar graph depicting the number of metastatic nodes in the lungs of control healthy mice and in lungs extracted from untreated and NRP1 treated C57BL/6 mice previously injected with B16-F10 cells intravenously. (D) Kaplan-Meier plot depicting the probability of survival of C57BL/6 mice with or without NRP1 inhibitor treatment after inoculation of $0.3X10^6$ B16-F10 cells subcutaneously. (E) XY plot depicting the volume of subcutaneous tumours in C57BL/6 mice with or without NRP1 inhibitor treatment after inoculation of $0.3X10^6$ B16-F10 cells subcutaneously.

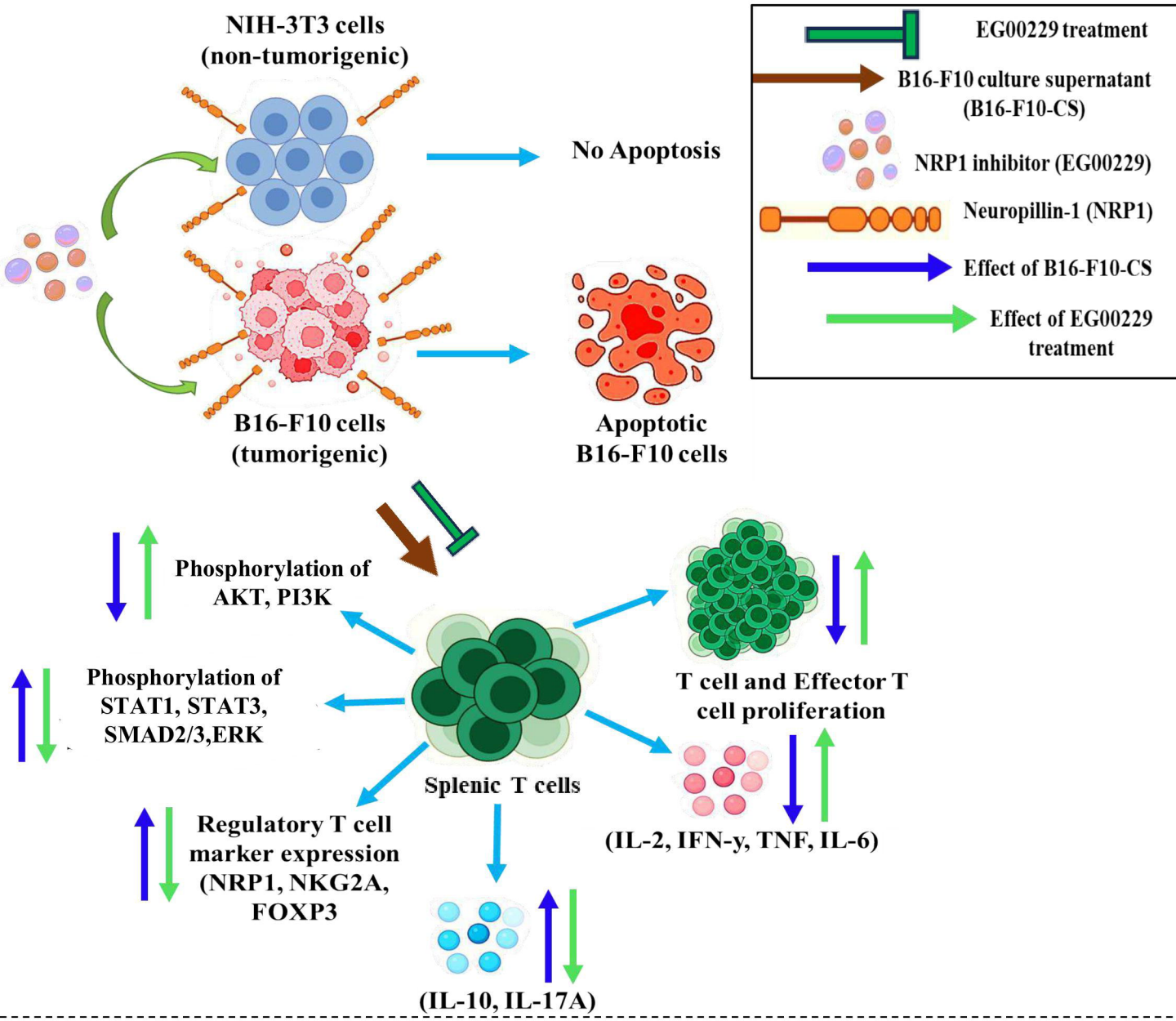
NIH-3T3 cells
(non-tumorigenic)
No Apoptosis
B16-F10 cells
(tumorigenic)
Apoptotic
B16-F10 cells
EG00229 treatment
B16-F10 culture supernatant
(B16-F10-CS)
NRP1 inhibitor (EG00229)
Neuropillin-1 (NRP1)
Effect of B16-F10-CS
Effect of EG00229
treatment
Phosphorylation of
AKT, PI3K
Phosphorylation of
STAT1, STAT3,
SMAD2/3,ERK
Regulatory T cell
marker expression
(NRP1, NKG2A,
FOXP3
Splenic T cells
T cell and Effector T
cell proliferation
(IL-2, IFN-y, TNF, IL-6)
(IL-10, IL-17A)

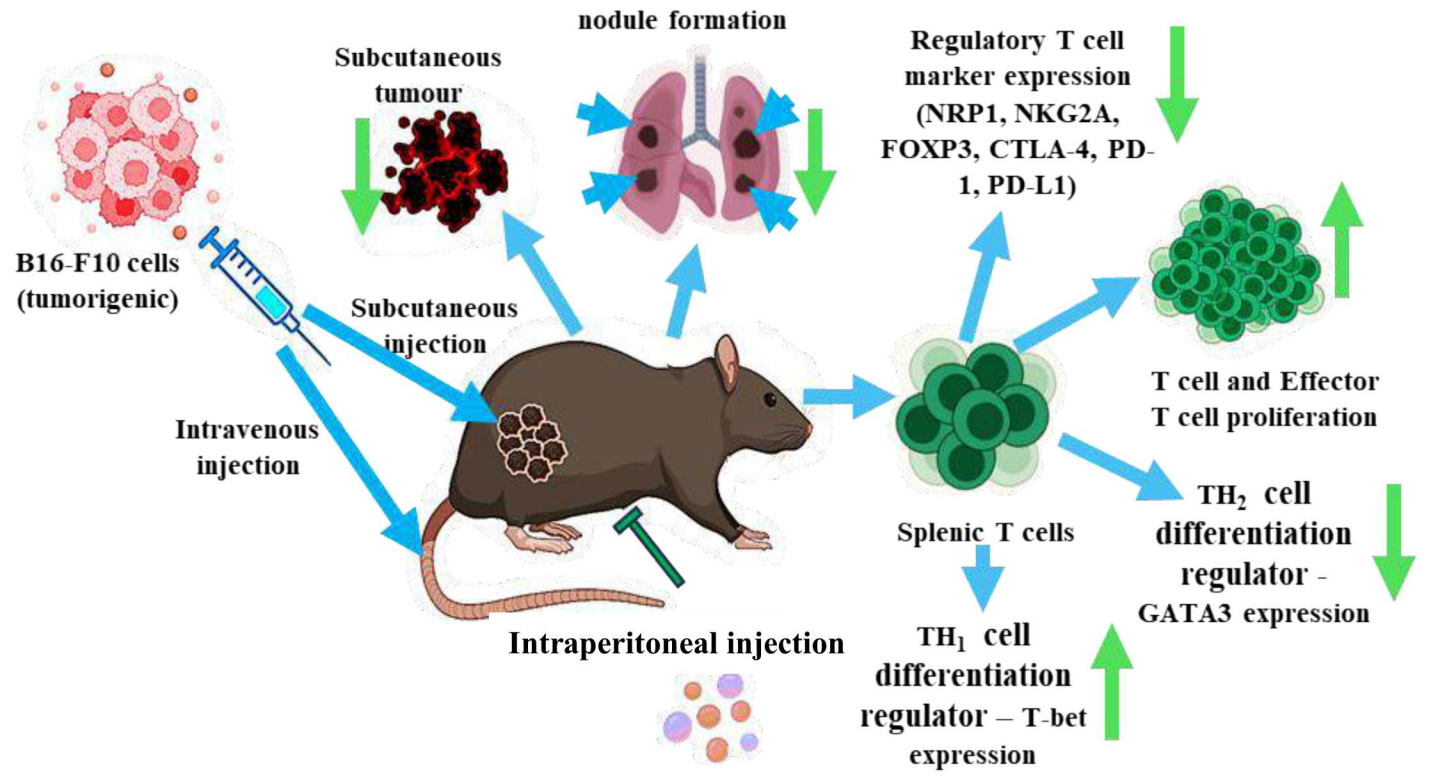
B16-F10 cells
(tumorigenic)
Subcutaneous
tumour
nodule formation
Subcutaneous
injection
Intravenous
injection
Intraperitoneal injection
Regulatory T cell
marker expression
(NRP1, NKG2A,
FOXP3, CTLA-4, PD-
1, PD-L1)
T cell and Effector
T cell proliferation
Splenic T cells
TH2 cell
differentiation
regulator -
GATA3 expression
TH1 cell
differentiation
regulator – T-bet
expression

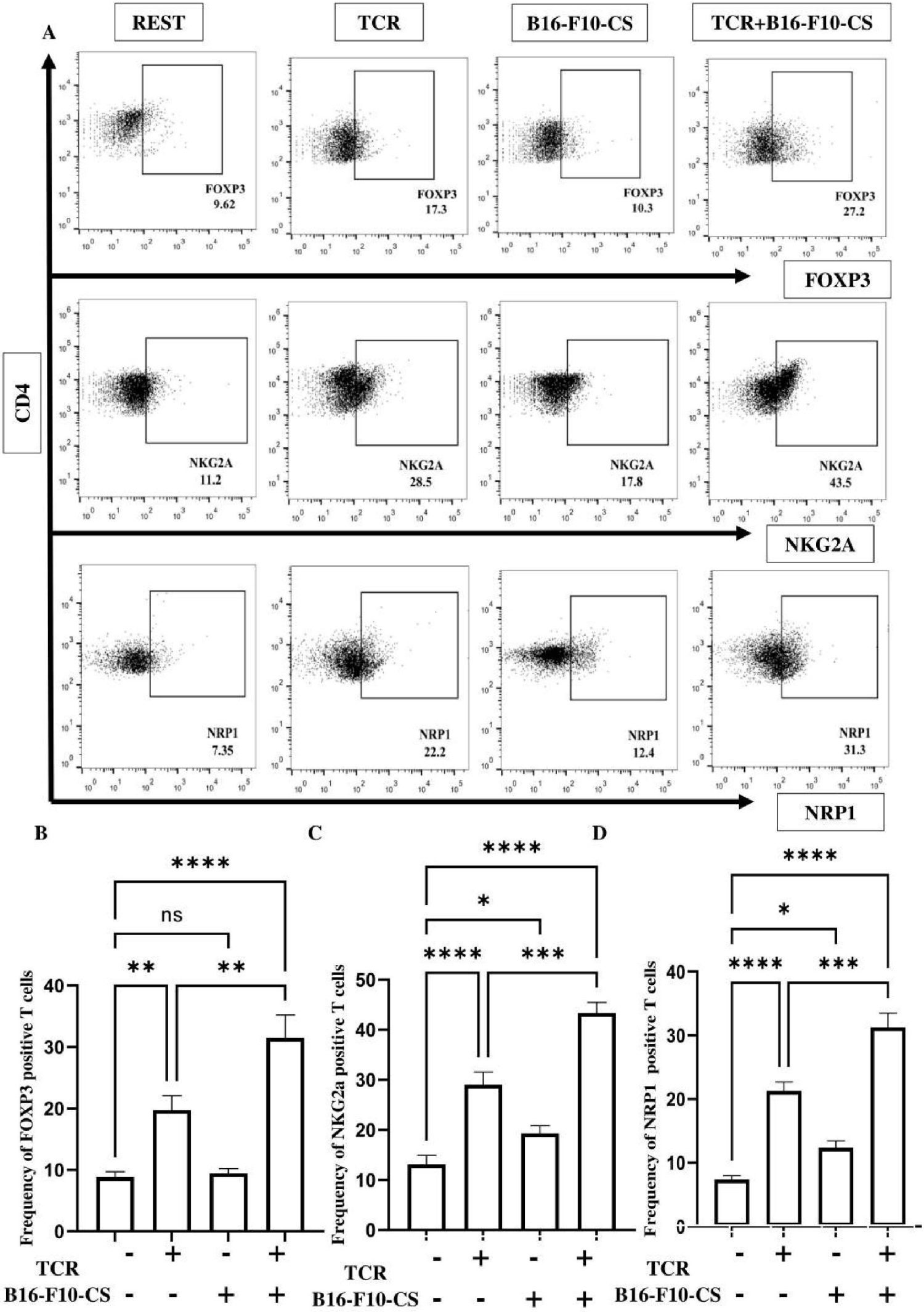
A
REST
TCR
B16-F10-CS
TCR+B16-F10-CS
FOXP3
9.62
FOXP3
17.3
FOXP3
10.3
FOXP3
27.2
FOXP3
CD4
NKG2A
11.2
NKG2A
28.5
NKG2A
17.8
NKG2A
43.5
NKG2A
NRP1
7.35
NRP1
22.2
NRP1
12.4
NRP1
31.3
NRP1
B
C
D
****
ns
**
**
Frequency of FOXP3 positive T cells
TCR
B16-F10-CS
****
*
****
***
Frequency of NKG2a positive T cells
TCR
B16-F10-CS
****
*
****
***
Frequency of NRP1 positive T cells
TCR
B16-F10-CS

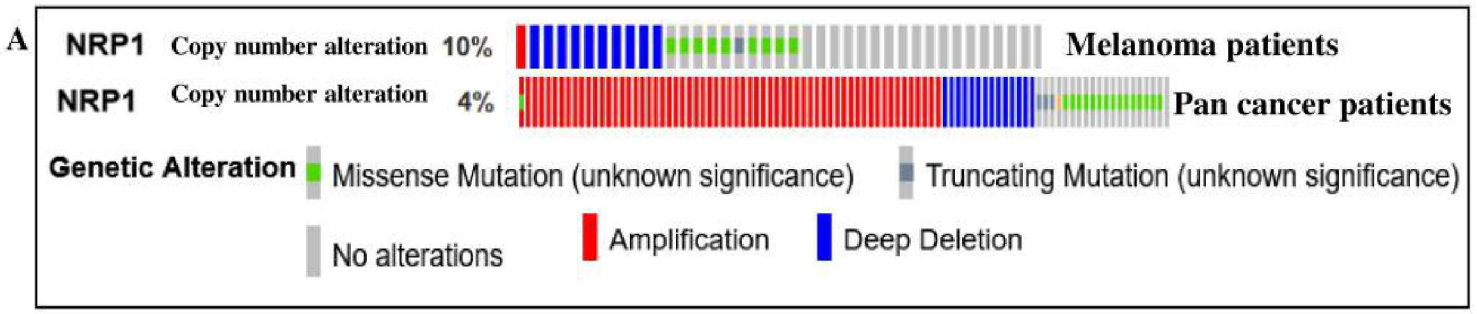
A
NRP1 Copy number alteration 10%
Melanoma patients
NRP1 Copy number alteration 4%
Pan cancer patients
Genetic Alteration
Missense Mutation (unknown significance)
Truncating Mutation (unknown significance)
No alterations
Amplification
Deep Deletion

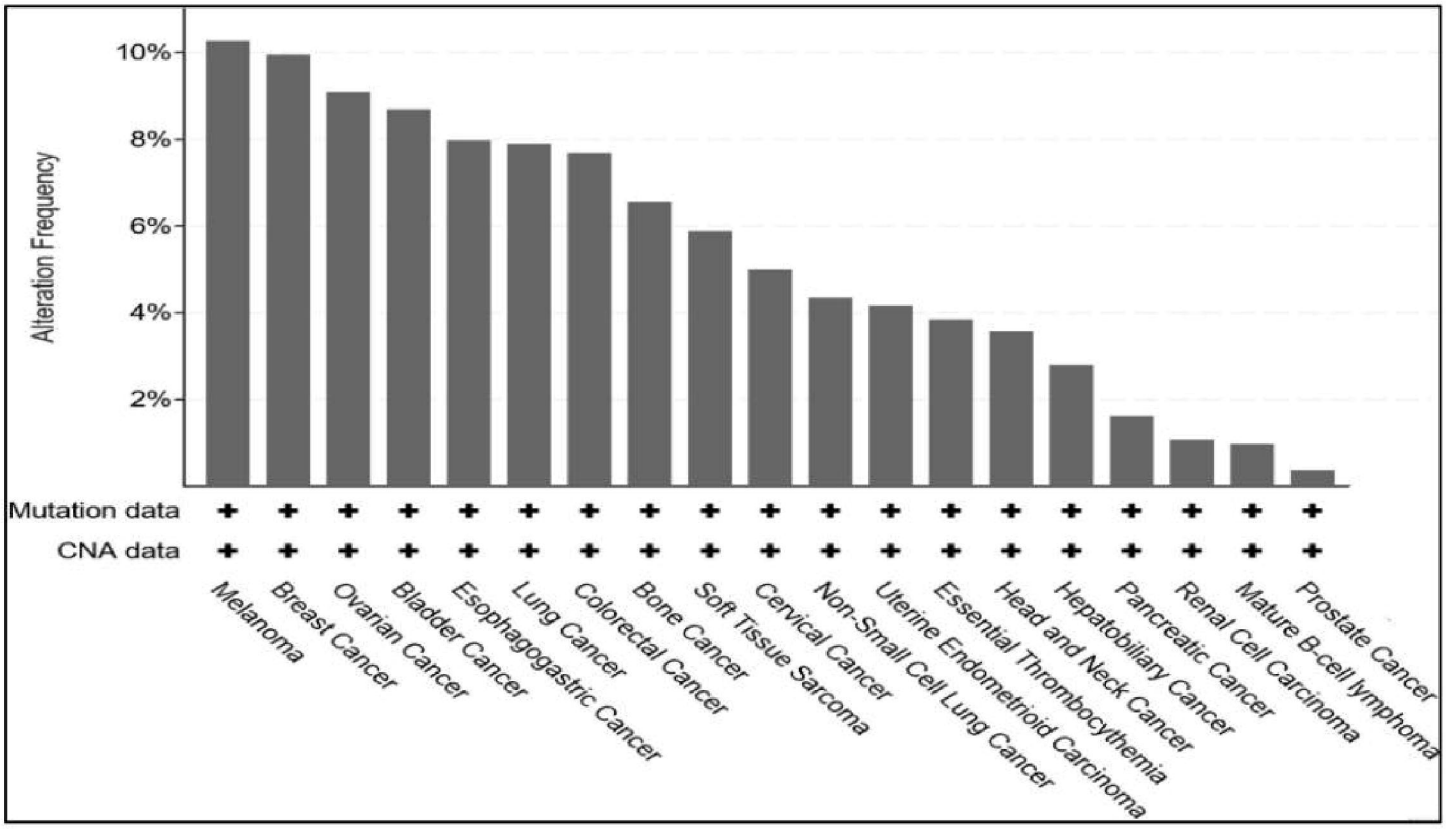
B
Alteration Frequency
10%
8%
6%
4%
2%
Mutation data
CNA data
Melanoma
Breast Cancer
Ovarian Cancer
Bladder Cancer
Esophagogastric Cancer
Lung Cancer
Colorectal Cancer
Bone Cancer
Soft Tissue Sarcoma
Cervical Cancer
Non-Small Cell Lung Cancer
Uterine Endometrioid Carcinoma
Essential Thrombocythemia
Head and Neck Cancer
Hepatobiliary Cancer
Pancreatic Cancer
Renal Cell Carcinoma
Mature B-cell lymphoma
Prostate Cancer

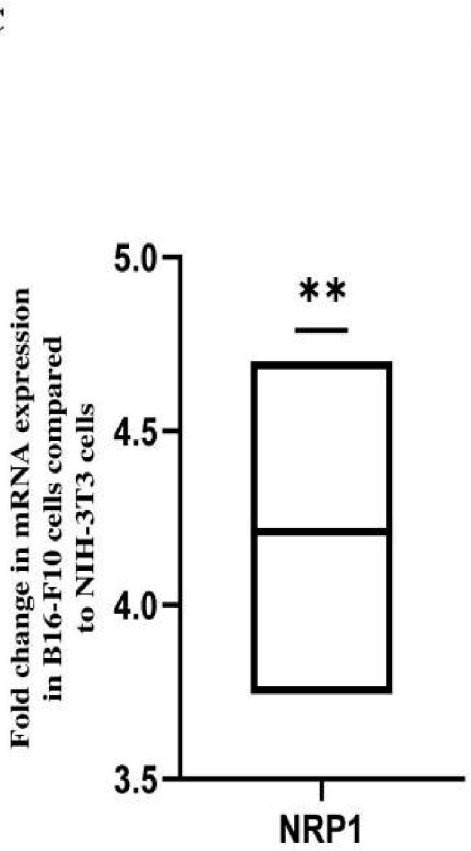
C
Fold change in mRNA expression in B16-F10 cells compared to NIH-3T3 cells
5.0
4.5
4.0
3.5
**
NRP1

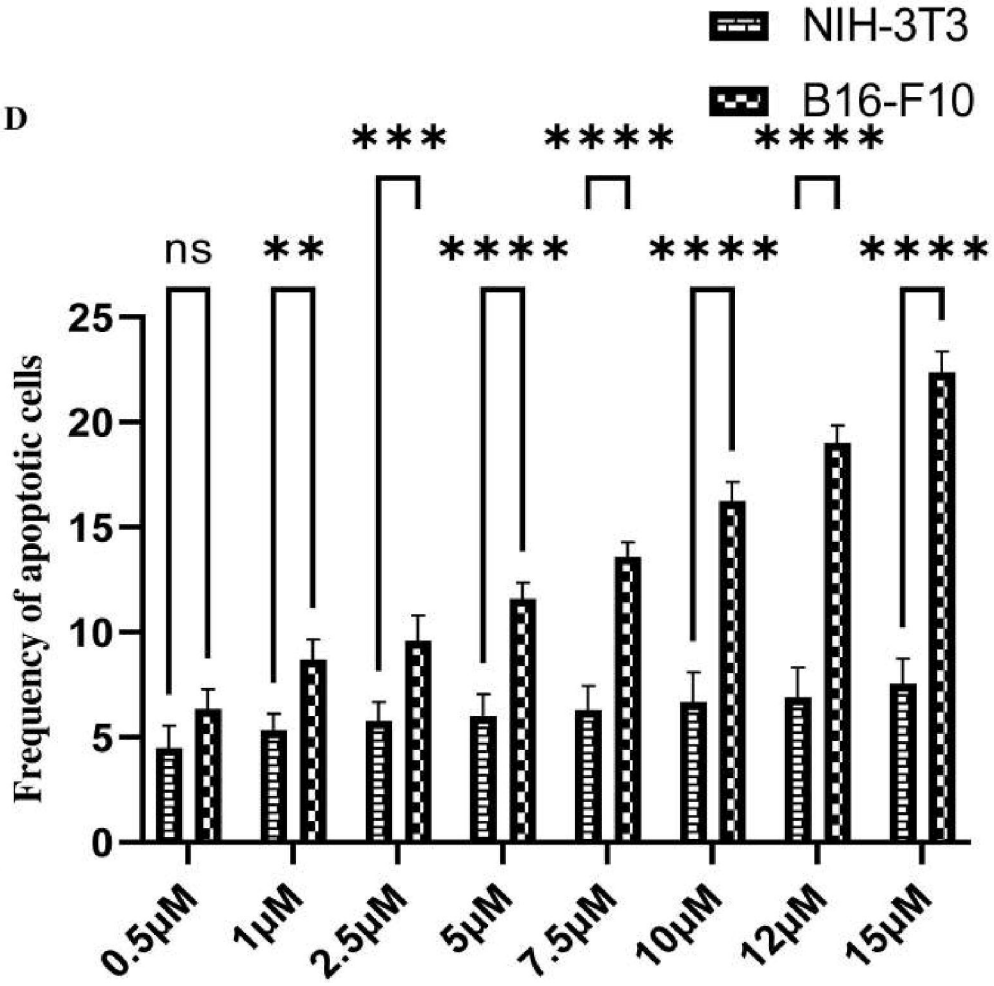
D
NIH-3T3
B16-F10
Frequency of apoptotic cells
25
20
15
10
5
0
ns
**
***
****
****
****
****
****
0.5μM
1μM
2.5μM
5μM
7.5μM
10μM
12μM
15μM

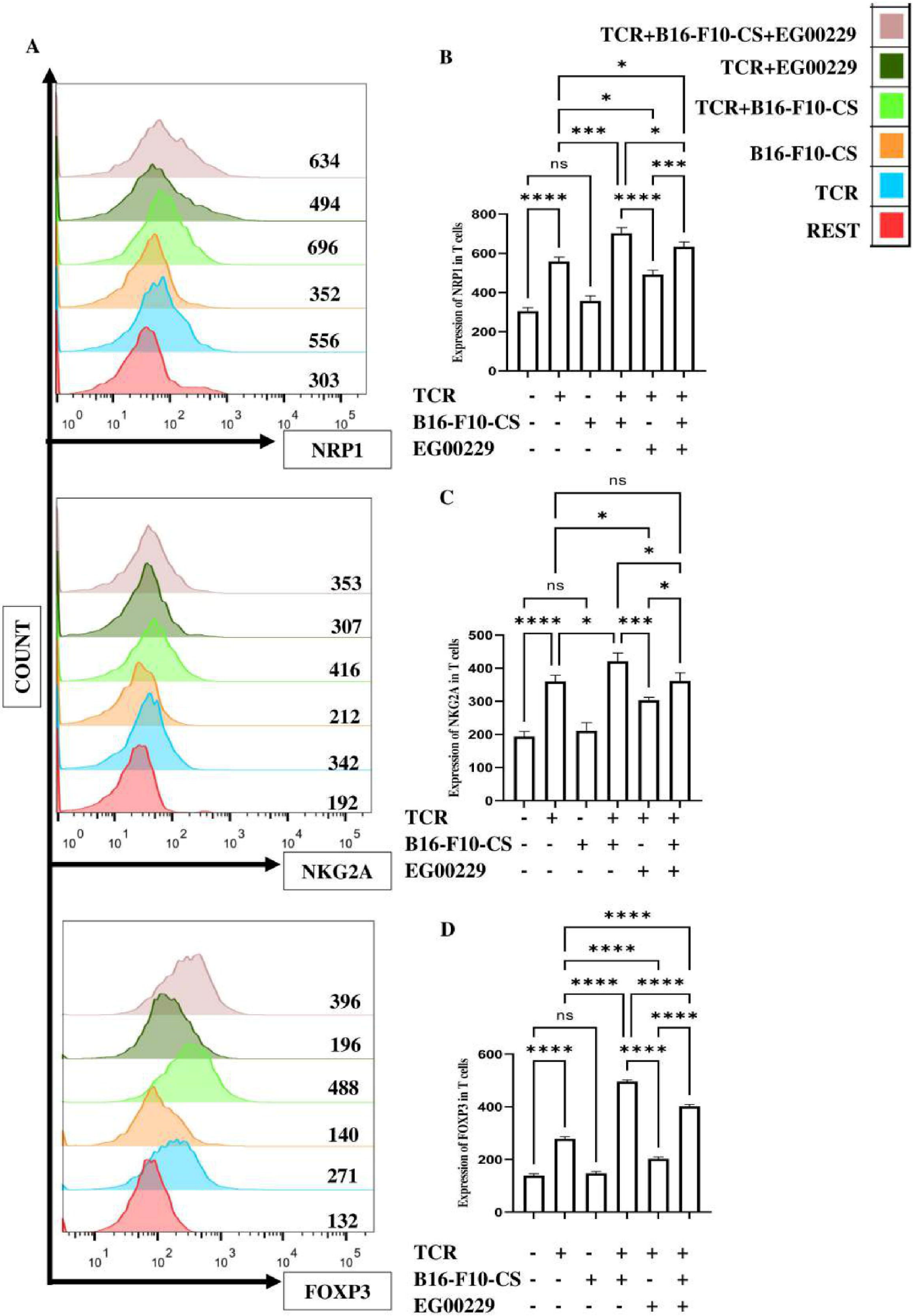
A
B
C
D
TCR+B16-F10-CS+EG00229
TCR+EG00229
TCR+B16-F10-CS
B16-F10-CS
TCR
REST
COUNT
NRP1
NKG2A
FOXP3
634
494
696
352
556
303
353
307
416
212
342
192
396
196
488
140
271
132
Expression of NRP1 in T cells
Expression of NKG2A in T cells
Expression of FOXP3 in T cells
TCR
B16-F10-CS
EG00229
ns
*
***
****

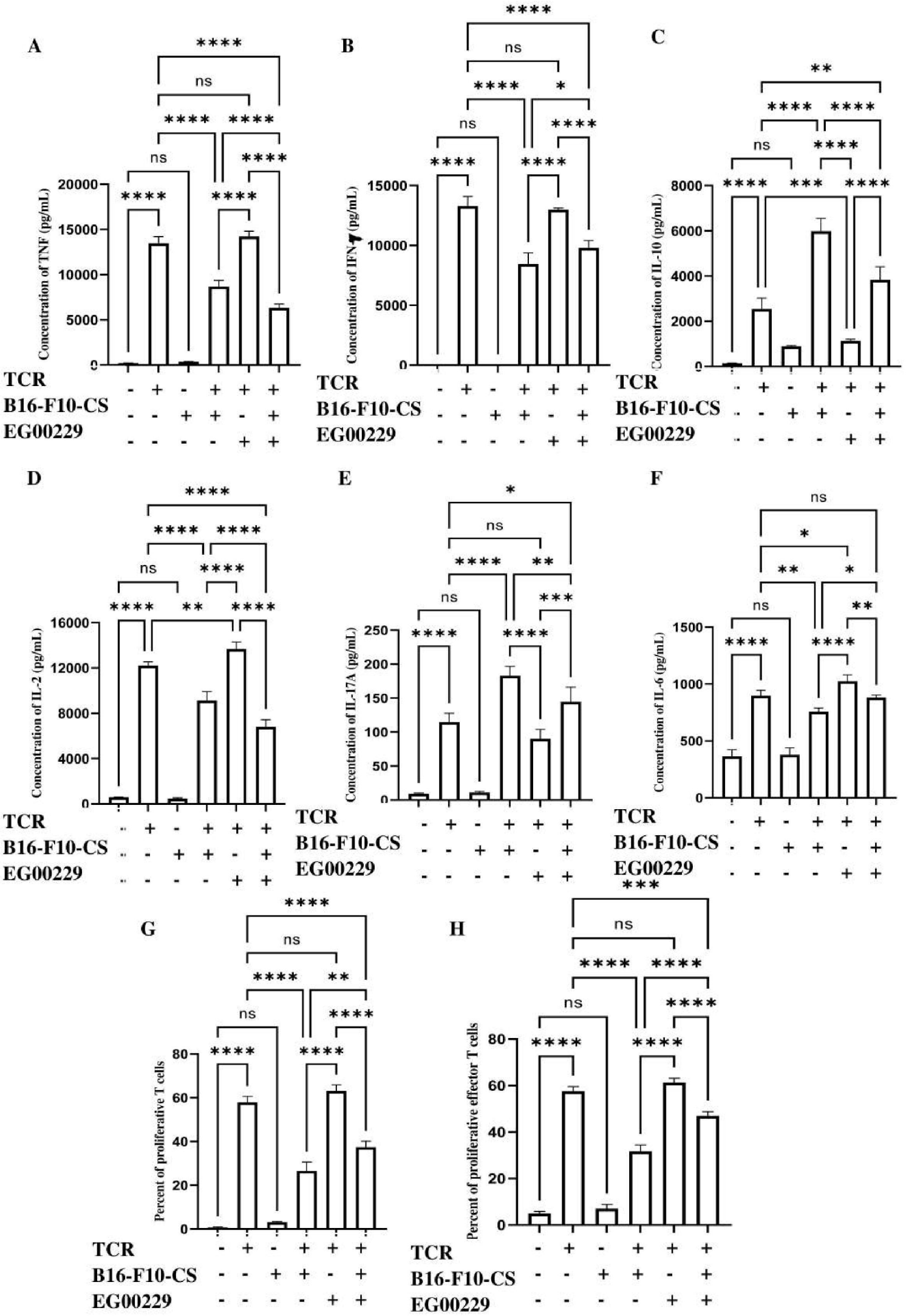
A
Concentration of TNF (pg/mL)
B
Concentration of IFN-γ (pg/mL)
C
Concentration of IL-10 (pg/mL)
D
Concentration of IL-2 (pg/mL)
E
Concentration of IL-17A (pg/mL)
F
Concentration of IL-6 (pg/mL)
G
Percent of proliferative T cells
H
Percent of proliferative effector T cells
TCR
B16-F10-CS
EG00229

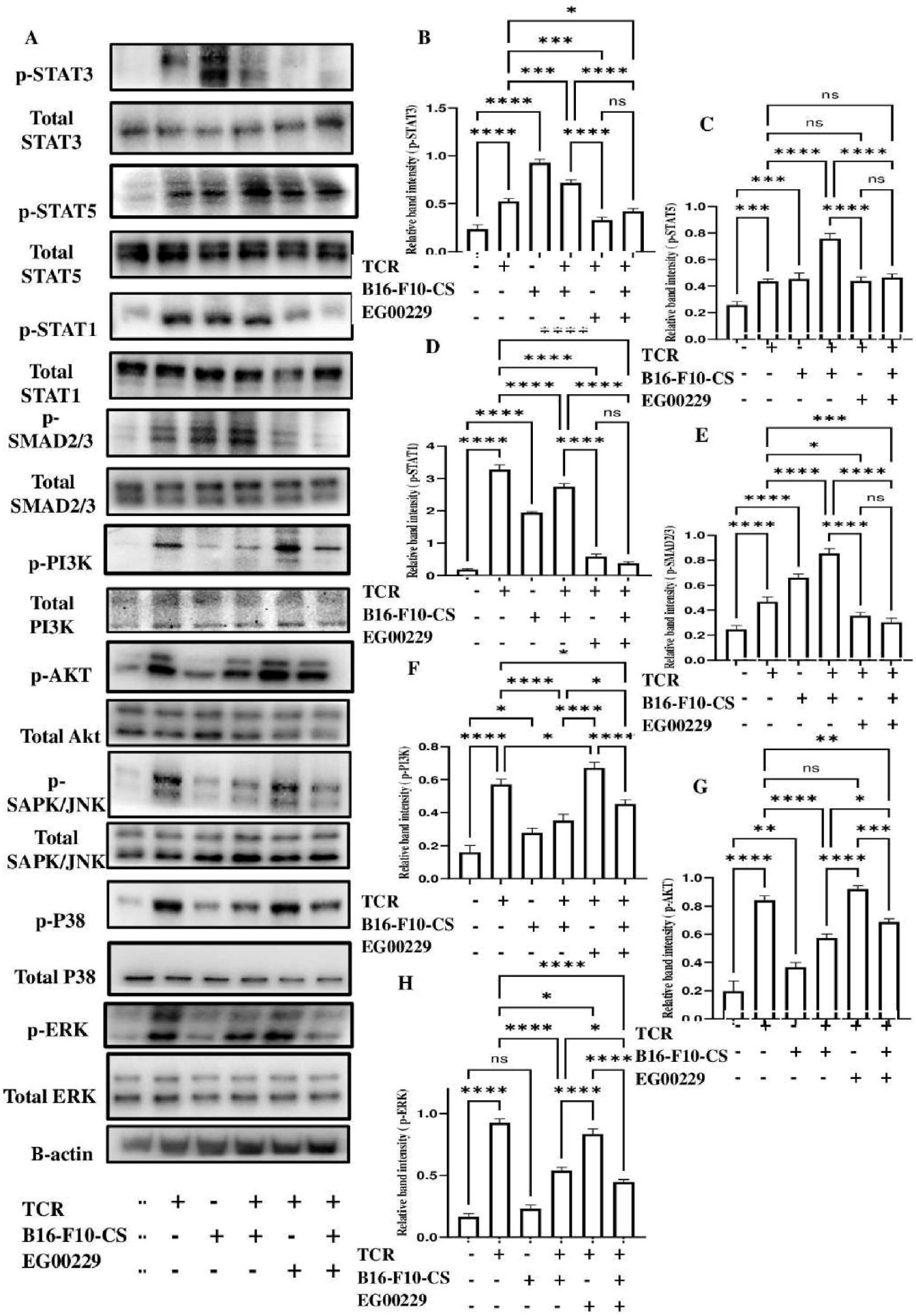
A
p-STAT3
Total STAT3
p-STAT5
Total STAT5
p-STAT1
Total STAT1
p-SMAD2/3
Total SMAD2/3
p-PI3K
Total PI3K
p-AKT
Total Akt
p-SAPK/JNK
Total SAPK/JNK
p-P38
Total P38
p-ERK
Total ERK
B-actin
TCR
B16-F10-CS
EG00229
B
Relative band intensity (p-STAT3)
C
Relative band intensity (p-STAT5)
D
Relative band intensity (p-STAT1)
E
Relative band intensity (p-SMAD2/3)
F
Relative band intensity (p-PI3K)
G
Relative band intensity (p-AKT)
H
Relative band intensity (p-ERK)
ns

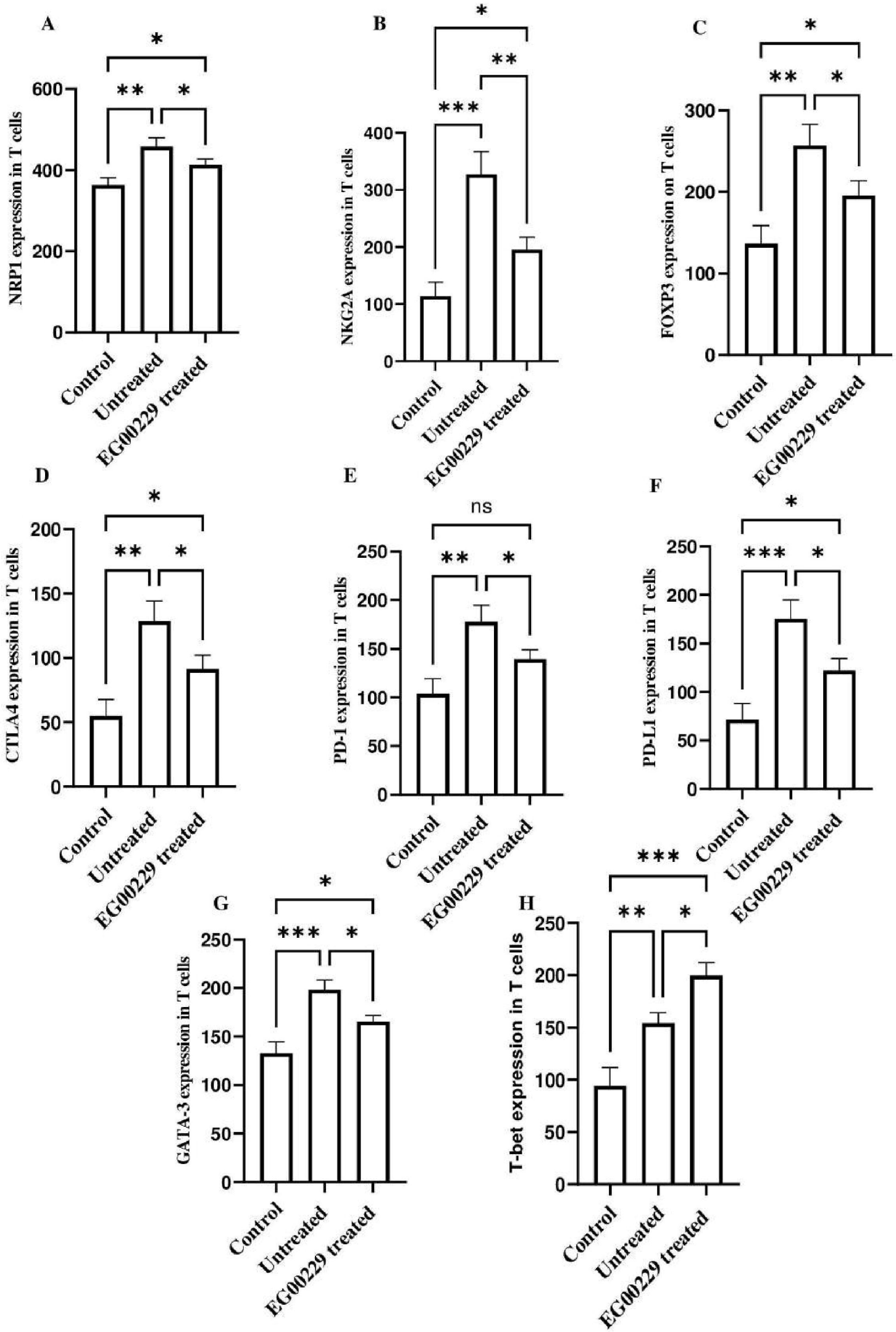
A
NRP1 expression in T cells
600
400
200
0
*
**
*
Control
Untreated
EG00229 treated
B
NKG2A expression in T cells
400
300
200
100
0
*
**
***
Control
Untreated
EG00229 treated
C
FOXP3 expression on T cells
300
200
100
0
*
**
*
Control
Untreated
EG00229 treated
D
CTLA4 expression in T cells
200
150
100
50
0
*
**
*
Control
Untreated
EG00229 treated
E
PD-1 expression in T cells
250
200
150
100
50
0
ns
**
*
Control
Untreated
EG00229 treated
F
PD-L1 expression in T cells
250
200
150
100
50
0
*
***
*
Control
Untreated
EG00229 treated
G
GATA-3 expression in T cells
250
200
150
100
50
0
*
***
*
Control
Untreated
EG00229 treated
H
T-bet expression in T cells
250
200
150
100
50
0
***
**
*
Control
Untreated
EG00229 treated

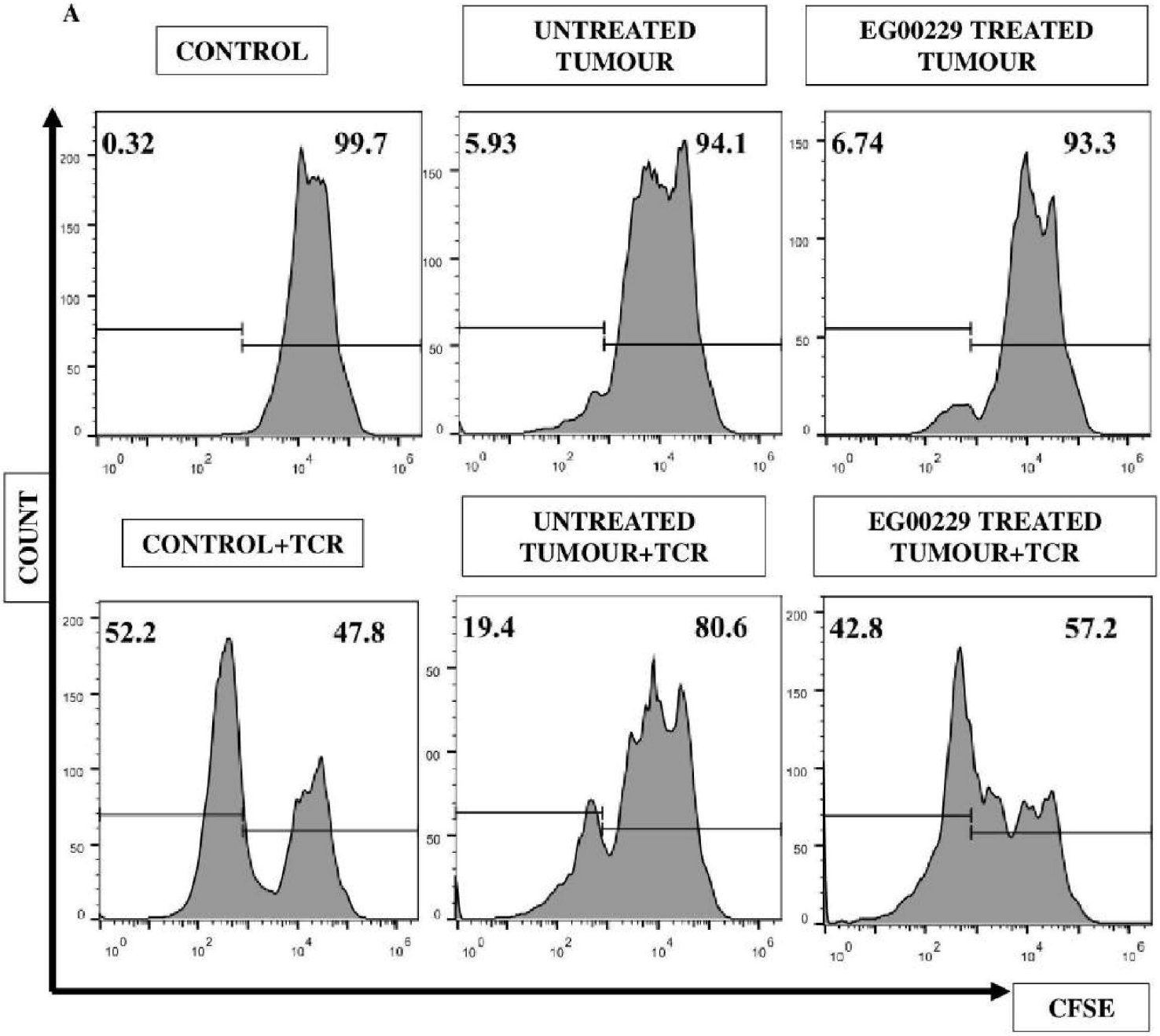
A
CONTROL
UNTREATED TUMOUR
EG00229 TREATED TUMOUR
0.32
99.7
5.93
94.1
6.74
93.3
CONTROL+TCR
UNTREATED TUMOUR+TCR
EG00229 TREATED TUMOUR+TCR
52.2
47.8
19.4
80.6
42.8
57.2
COUNT
CFSE

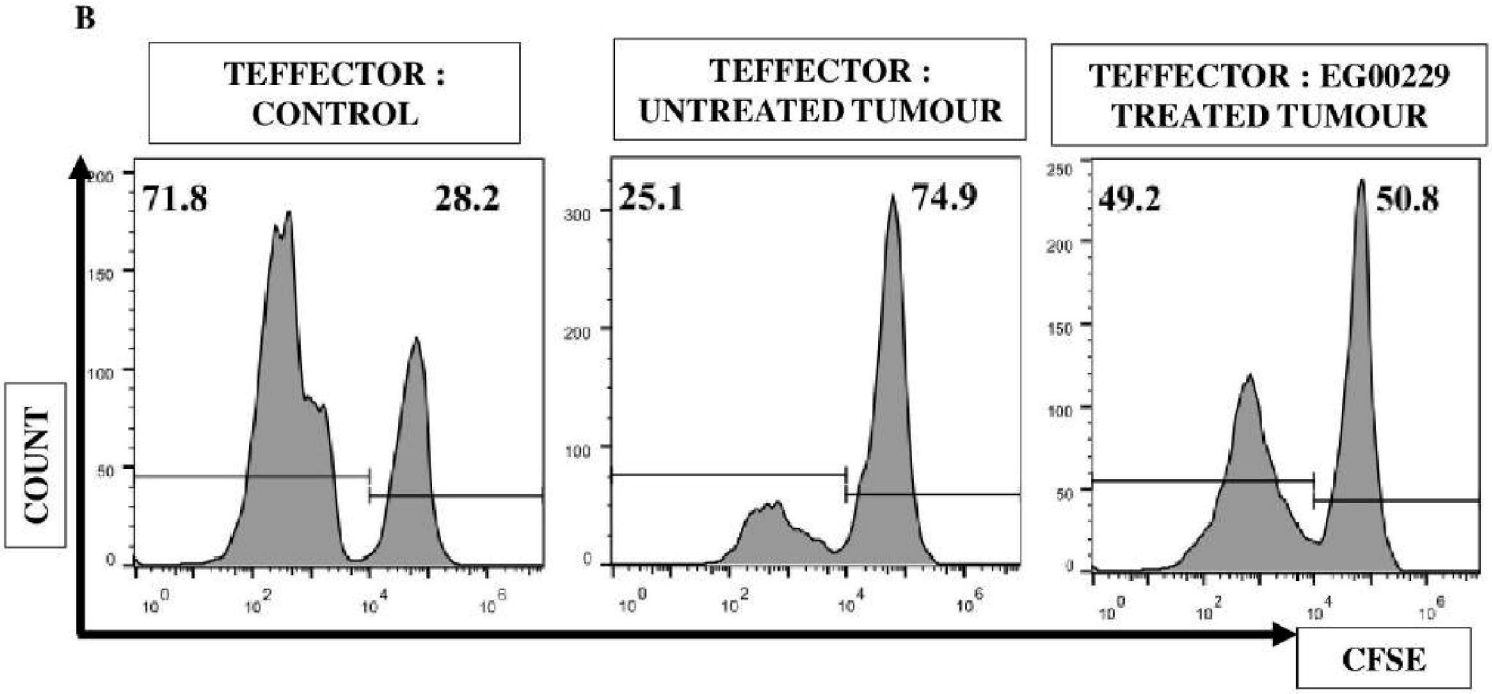
B
TEFFECTOR : CONTROL
TEFFECTOR : UNTREATED TUMOUR
TEFFECTOR : EG00229 TREATED TUMOUR
71.8
28.2
25.1
74.9
49.2
50.8
COUNT
CFSE

A

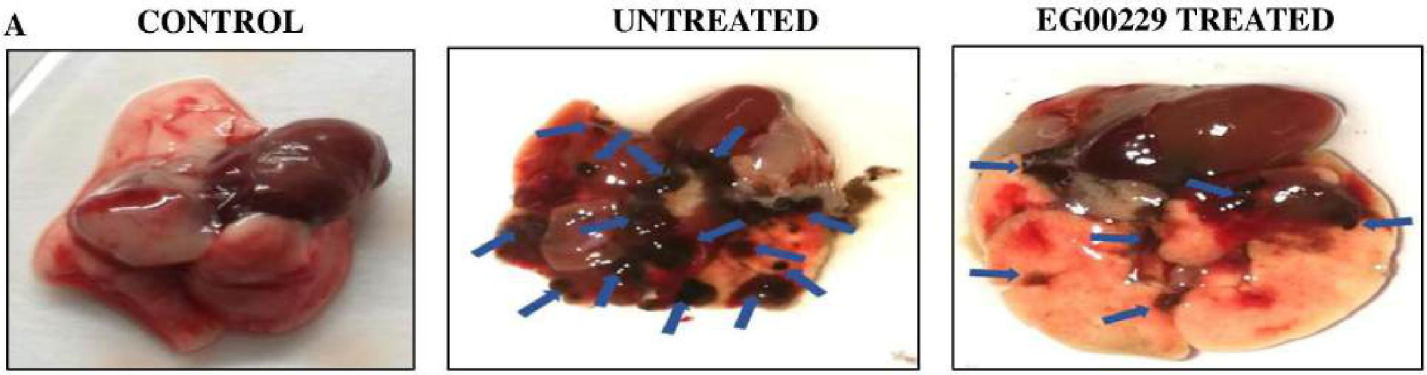
CONTROL
UNTREATED
EG00229 TREATED

B

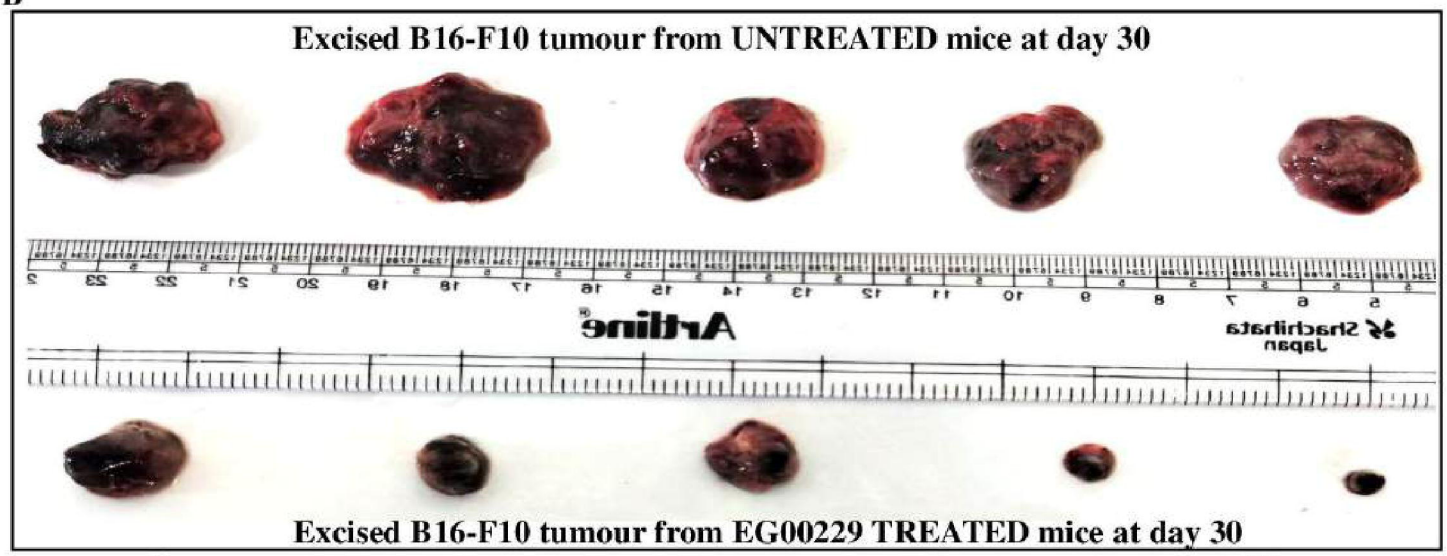
Excised B16-F10 tumour from UNTREATED mice at day 30
Excised B16-F10 tumour from EG00229 TREATED mice at day 30

C

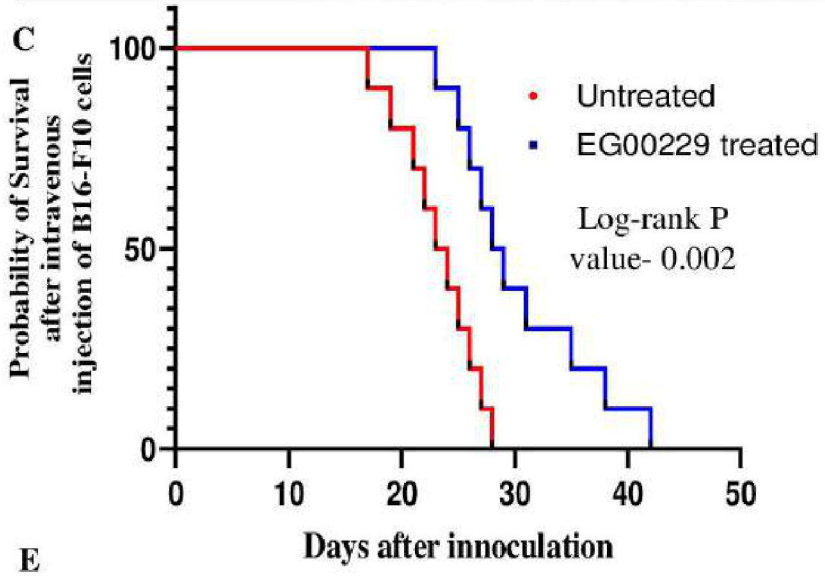
Probability of Survival after intravenous injection of B16-F10 cells
100
50
0
0
10
20
30
40
50
Days after innoculation
Untreated
EG00229 treated
Log-rank P value- 0.002

D

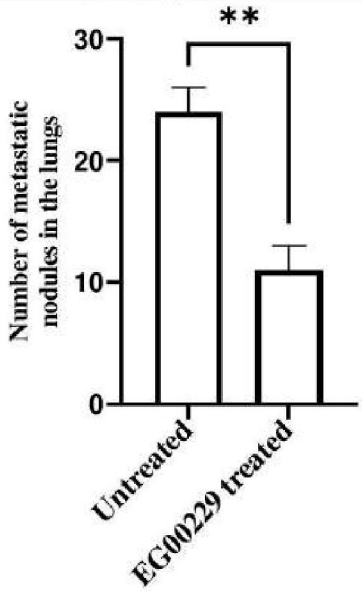
**
Number of metastatic nodules in the lungs
30
20
10
0
Untreated
EG00229 treated

E

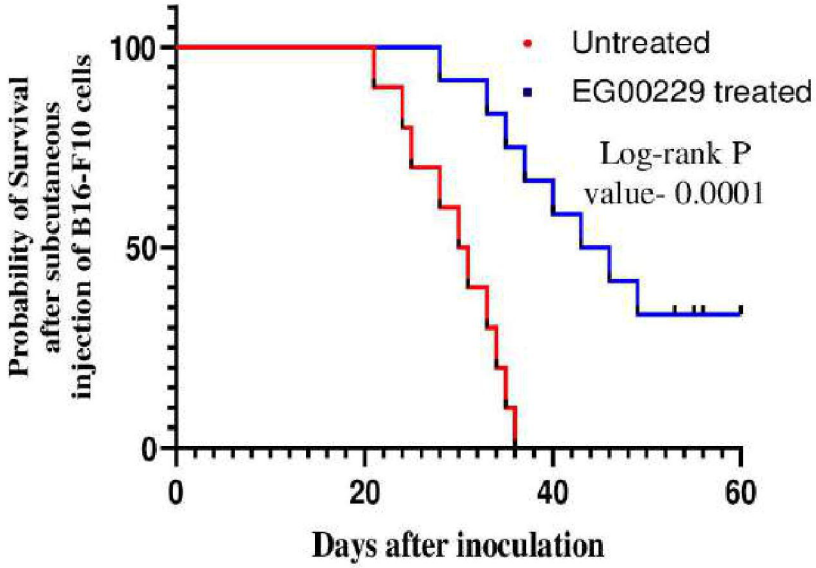
Probability of Survival after subcutaneous injection of B16-F10 cells
100
50
0
0
20
40
60
Days after inoculation
Untreated
EG00229 treated
Log-rank P value- 0.0001

F

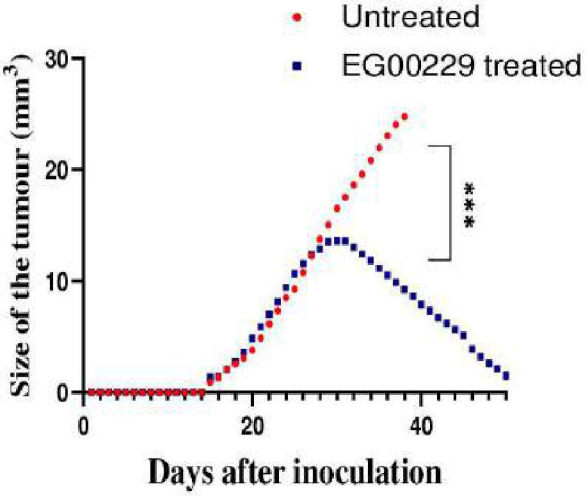
Size of the tumour (mm^3)
30
20
10
0
0
20
40
Days after inoculation
Untreated
EG00229 treated
***